Tomographic Diffractive Imaging

Three-dimensional reconstruction of the charge density of non-periodic objects from their X-ray diffraction pattern intensities .

J. Spence, M.Howells, H. He, S.Marchesini, U.Weierstall, H.Chapman.
ASU Physics, LBL, LLL. DOE, ARO $.

Science requires new methods for tomographic imaging of nanostructures at high resolution.

Leucippus, Greek Philosopher (450 BC)
- “there is a smallest fragment”

Democritis (470-380 BC)of Abdera
- cult of “Atomism”.
“Atomists” believed that there were several indivisible fragment (“atoms”, fundamental particles),
which combined in various ways to produce the different varieties of bulk matter.

All described by the Roman poet Titus Lucretius Carus (95 BC) in “De Rerum Natura”
(“On the nature of things”)

?
Robert Hooke, 1665 - facets.
Micrographica

Prout, 1805

Why lensless imaging ?

- A technique for 3D imaging of 0.5 – 20 μm isolated objects
- Too thick for EM.
- Too thick for zone-plate tomographic X-ray microscopy (depth of focus < 1 μm at 10 nm resolution for soft X-rays even if zone plates become available)
- Provides a general method of imaging with any radiation for which lenses don't exist (neutrons, coherent atoms..). Each has different interaction giving new info.

Goals

- <10 nm resolution (3D) in 1 - 10μm size biological specimens
  (small frozen hydrated cell, organelle; see macromolecular aggregates)
  Limitation: radiation damage!

- < 2 nm resolution in less sensitive nanostructures
  (Inclusions, porosity, clusters, composite nanostructures, aerosols…)
  eg: molecular sieves, catalysts, crack propagation, mesoporous structures

First atomic-resolution diffractive image reconstruction.

Double-walled Nanotube

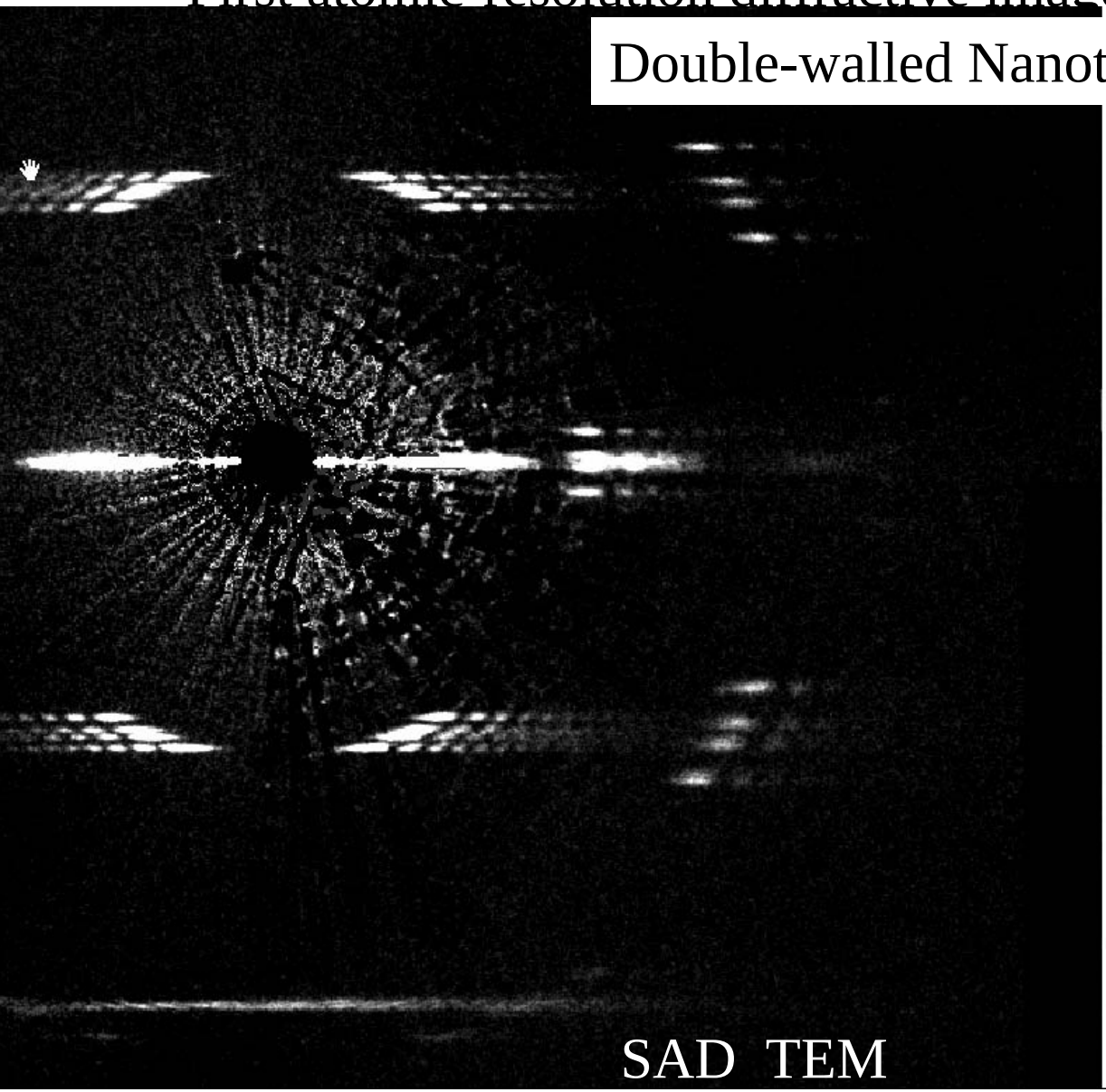

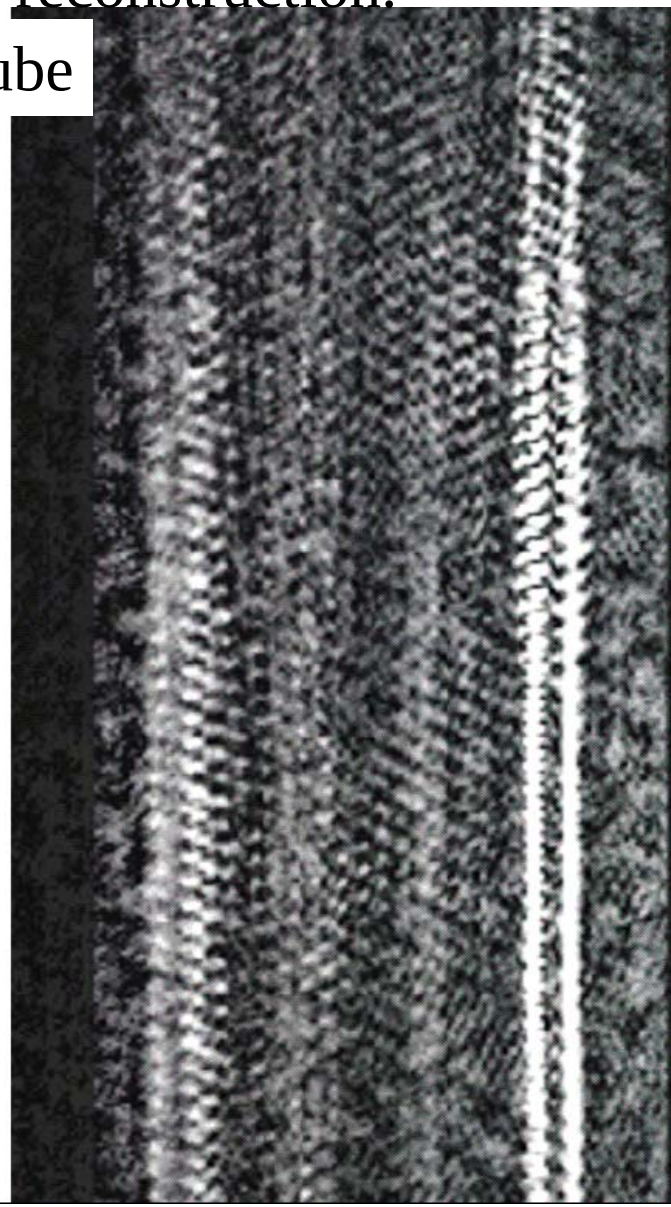

Image reconstructed from electron-diffraction pattern by HiO

Requires image plate, not CCD.

J.M.Zuo et al Science 300, 1420 (2003).

Tutorial on coherence.

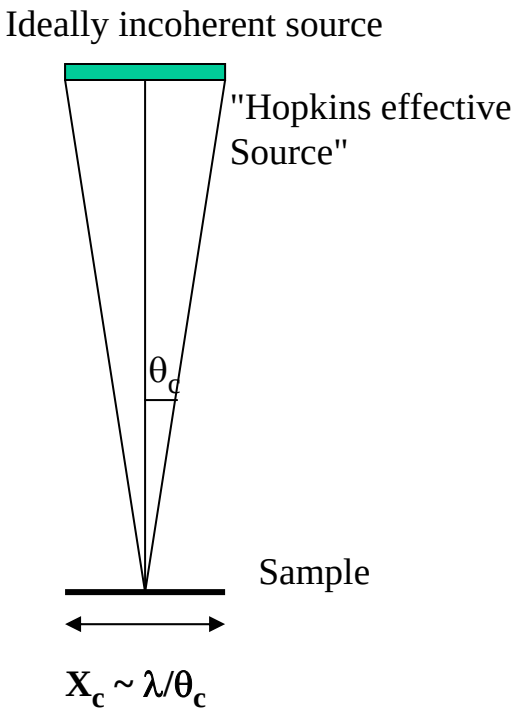

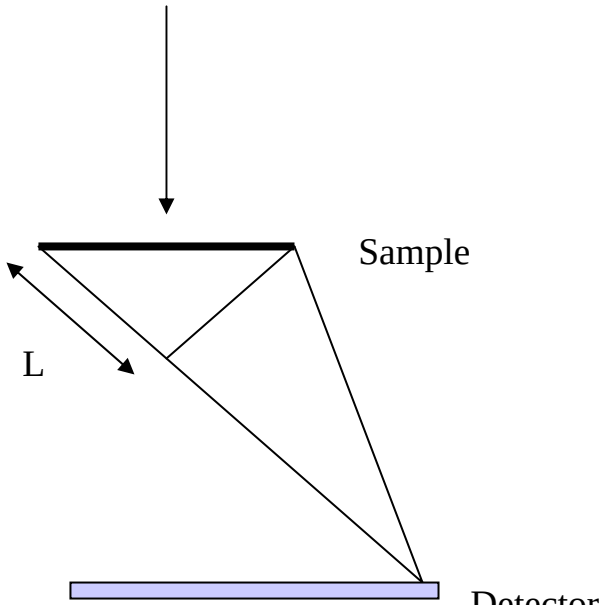

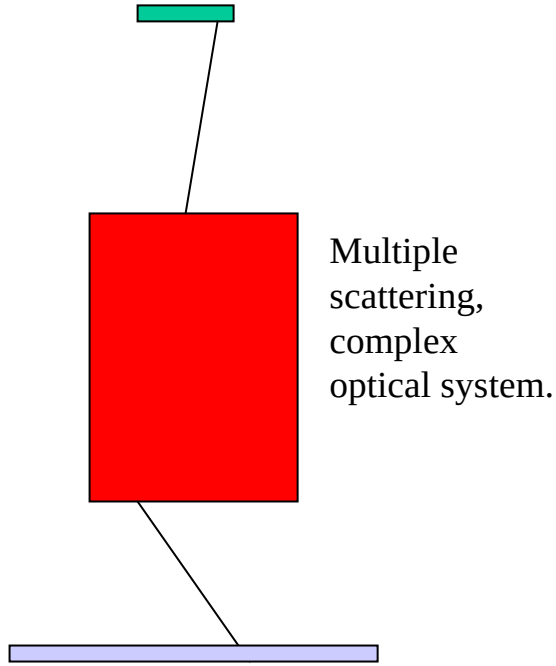

Spatial coherence across the beam
Need X_c > object for CXDI.

Longitudinal coherence $L_c = \lambda\ (E/\Delta E)$
Need $L_c > L$ for CXDI

General problem: Calculate *intensity* at detector for each source point and sum (recording time longer than $T_c = L_c/c$)

Coherence is the ability of a wavefield to interfere with itself. Each photon interferes only with itself.
Young's pinholes measure largest lateral separation X_c at which waves can interfere.
Waves of different frequency can interfere for the duration of the inverse beat frequency.
For Bragg scattering, spatial coherence must exceed xtal repeat distance (then $\Theta_c < \Theta_B$). For CXDI, X_c > object

The basic idea - "oversampling" solves the phase problem. **1. Collecting all the information.**

Shannon's theorem : All the info. in **diffuse** scattering is collected if it's sampled at "half the Bragg angle". Explain this…...

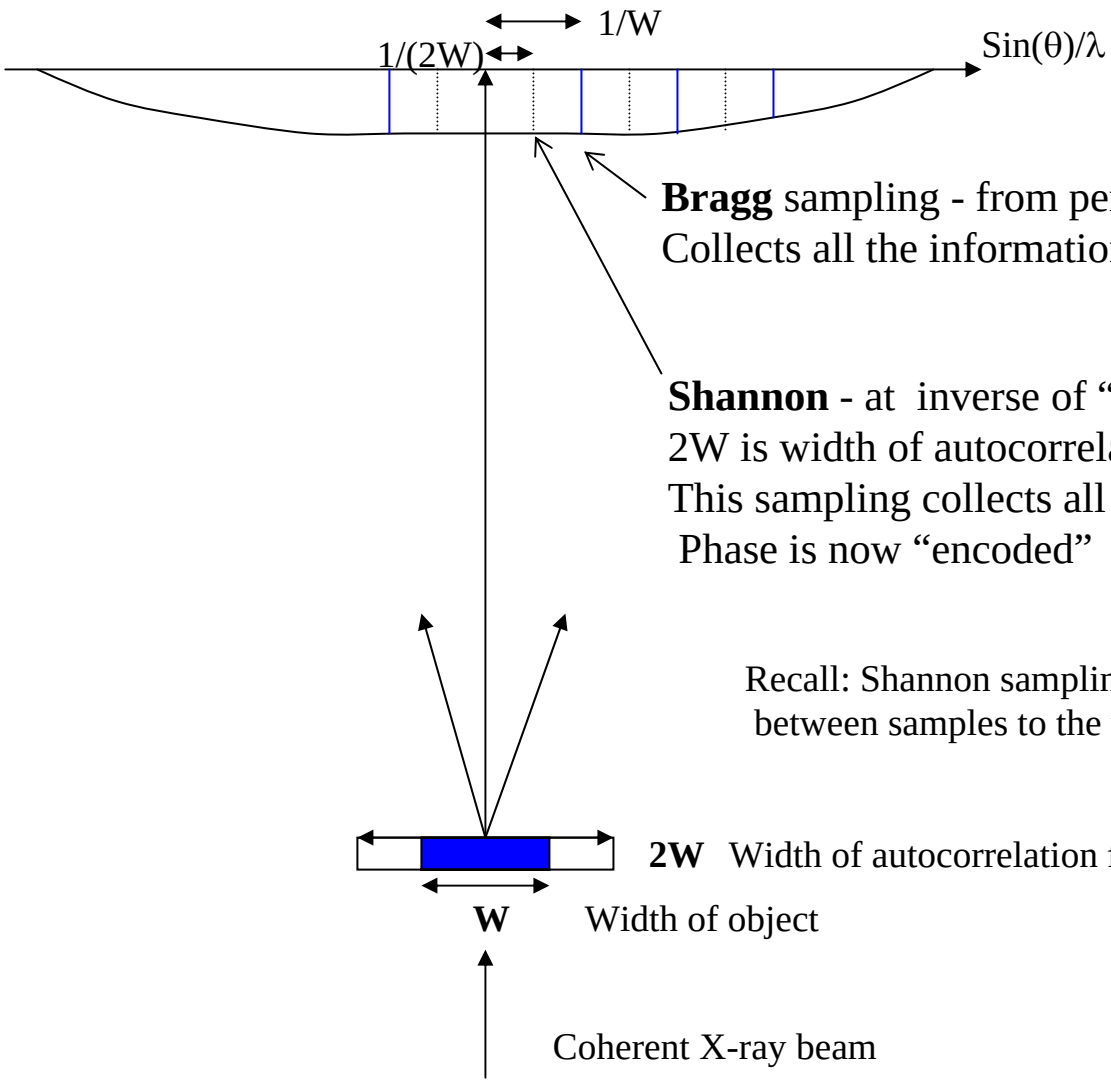

Bragg sampling - from periodic repetition of object, width W.
Collects all the information if amplitude **and phase** are recorded.

Shannon - at inverse of "bandlimit" 2W for diffracted INTENSITY.
2W is width of autocorrelation of object, which acts as "bandlimit".
This sampling collects all the info. if only **intensity** is detected.
Phase is now "encoded" in the intensity.

Recall: Shannon sampling of a bandlimited function allows interpolation between samples to the value of the continuous function.

"collect all info" means **number of eqns = number of unknowns**

In practice….

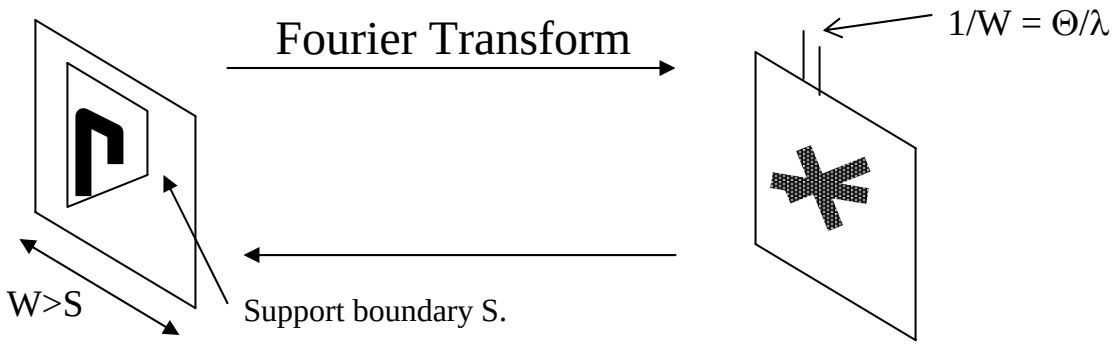

Object Diffraction pattern - diffuse

Iterate between object and diffraction pattern, overwriting known info in each space.

1. Start with measured diffraction amplitudes, random phases.
2. Transform to real space. Set object to zero outside known boundary (“support constraint”).
3. Make positive charge density zero. ("Sign constraint").
4. Transform to reciprocal space. Replace amplitudes with measured values. Keep old phases.
5. Go to 2.

With feedback, this is the “hybrid input-output” HiO algorithm of Feinup, Gerchberg, Saxton.

Also called oversampling (Sayre, Miao, Bates). Then **No. of eqns = No. of unknown phases**.

Diffract from region twice as big as object. Known half compensates for unknown phases.

For details see Weierstall et al Ultramic. 90, p. 171 (2002).

The basic idea - "oversampling" solves the phase problem. **2. Extracting the phases**.

Shannon sampling makes the number of Fourier eqns (one for each sample) equal to the number of unknown phases, hence inversion may be possible.

Are these eqns linear ? Independent ? . Linear once estimated phases supplied.

In real-space, this "oversampling" (w.r.t Bragg sampling) surrounds the isolated object by a border of **known**, zero charge density. (cf padding out with zeros).

Phases are found using Fienup-Gerchberg-Saxton (HiO) iterative algorithm. Convergence properties have been studied in detail. (Err Red error cannot increase. Projections convex sets).

Information needed for convergence; 1. The Fourier modulii. 2. The sign of the charge density 3. Approx boundary of the object (the support). (We have recently removed the need for this).

"Solves" **global optimization problem** (10^6 adjustable params !). Why does it work ?
- Fourier modulus constraint is not convex, **knowledge of phase is convex**.

Is the inversion unique ? (not in 1D. Yes in practice in 2D. Excellent in 3D).

Phase in physics. Bohr, Dirac, Squid, A/B effect, phase cooper-pair wavefunction ?

**

The basic idea - "oversampling" solves the phase problem. **3. History of ideas.**

1. D.Sayre. 1952 (BoyesWatson'47). "**Bragg sampling undersamples** autocorrn fn of molecules in a xtal".

2. Gerchberg and Saxton 1971. First **iterative algorithm**. Applied to electron diffraction data.

3. Fienup 1982. Adds feedback, support constraint to G-S. **HiO.** Works ! ("real" object, small phase shifts)

4. Bates, Fiddy, Youla, Yu,Bruck,Sodin, Barakat - uniqueness, convergence. **Projections on convex sets.**

5. Fienup. 1987. HiO for complex object with disjoint support. (Large phase shifts, multiple scattering)

5. Millane review article 1990. Widely read.

6. Miao et al 1999. Experimental soft-Xray images from diffraction patterns. Low res image used for support, beam stop.

7. Ian Robinson et al. 7.5 kV at APS (2001). Gold nanoxtals. Use shape transform around Braggs.

7 Weierstall et al 2002. First inversion of coherent electron diffraction patterns. Zuo:atomic resolution HiO.

**

First atomic-resolution image of a DWNT by any method.

Obtained by HiO. Aberration-free.

Gives ID, OD, Chiral vectors.

Zuo et al
Sceince 2003.

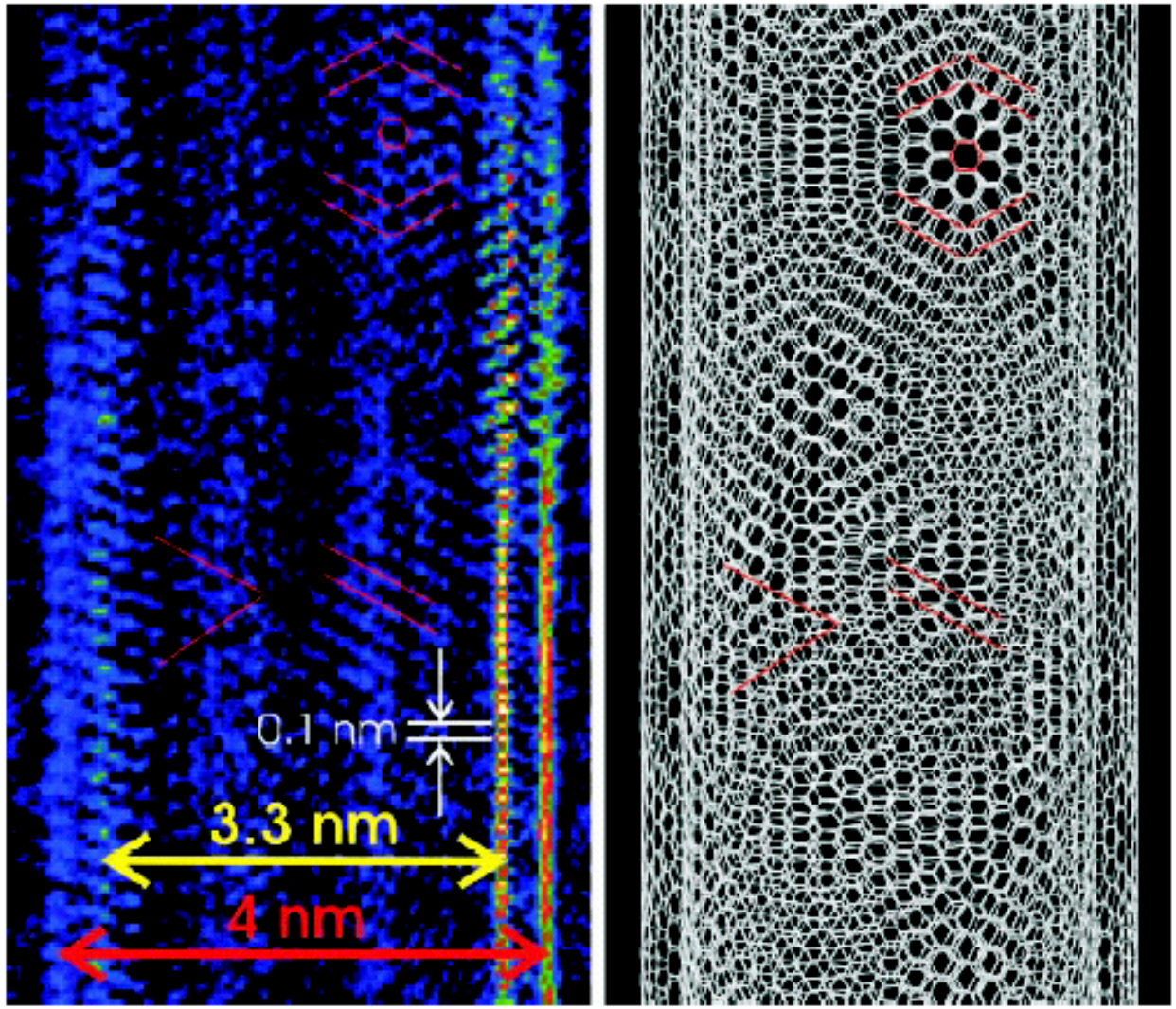

Fig. 2. (**left**) A section of the reconstructed DWNT image at 1-Å resolution and (**right**) a structural model constructed with the use of the chiral vectors of (35, 25) and (26, 24) that were determined from the image and diffraction pattern. The DWNT imaged here is one of many in our catalytic chemical vapor deposition–grown samples. Yellow and red lines mark the diameters of the inner and outer tubes, respectively. One side of walls is stronger than the other, which is because of the illumination. The DWNT is incommensurate. In projection, the structure has complex patterns showing both accidental coincidences and Moiré fringes, which are highlighted by hexagons and lines.

Atomic-resolution diffractive imaging with electrons using a TEM.

Zuo, Vartanyants et al Science, 300 1419 (2003)

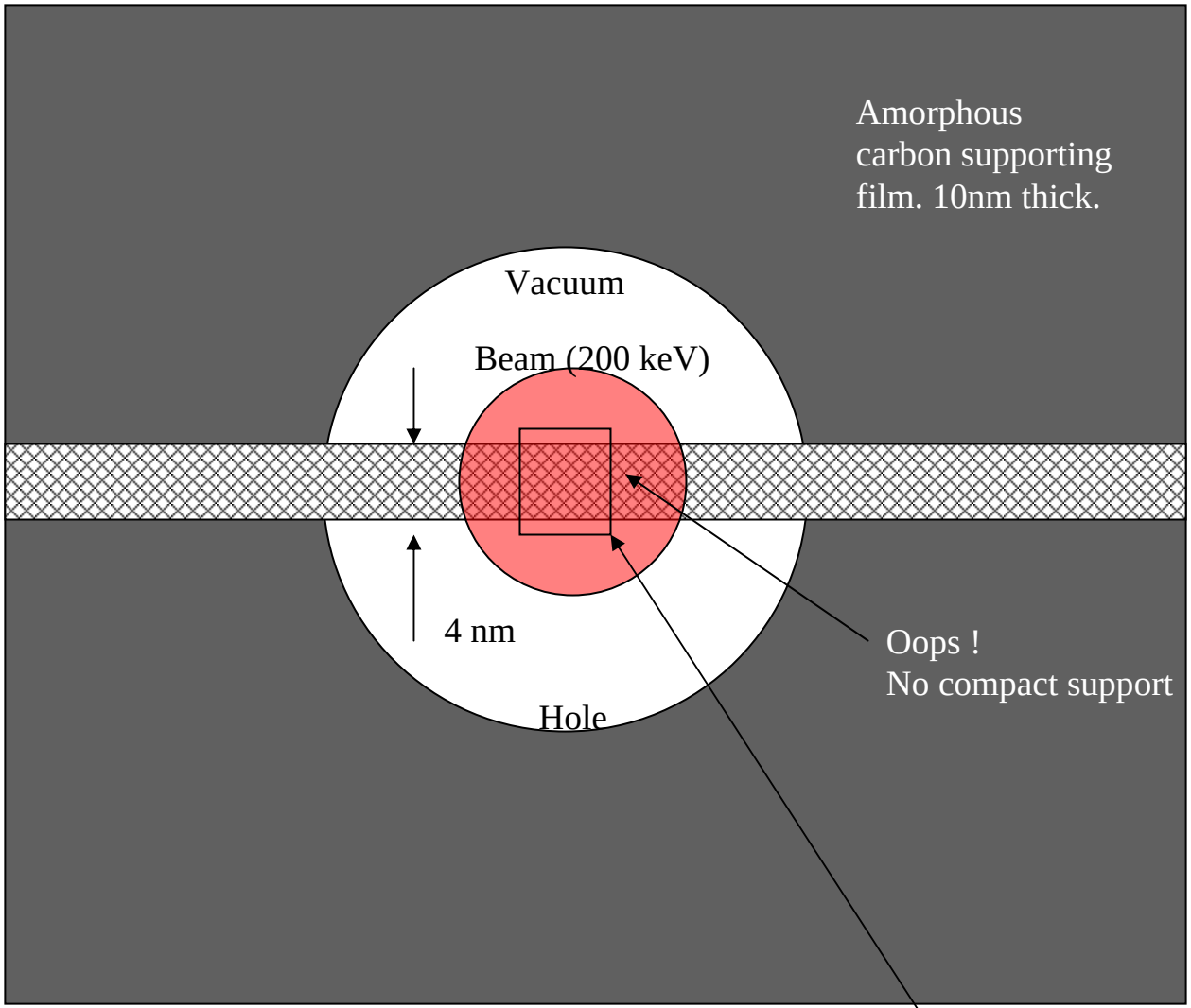

Coherent, high-energy electron **beam normal to page.**

The competition from HREM and STEM

Tomography in STEM with 1nm diameter electron probe.

QuickTime™ and a
decompressor
are needed to see this picture.

Catalyst particles. Red are Pt particles
on Alumina crystal. Fringes are Moire.
Resolution about 1nm. HAAD. Like STXM.
100 keV. P.Midgely et al, 2002

Current best HREM resolution is 0.78 Angstroms.

Gate Oxide ~ 5 Si Atoms thick

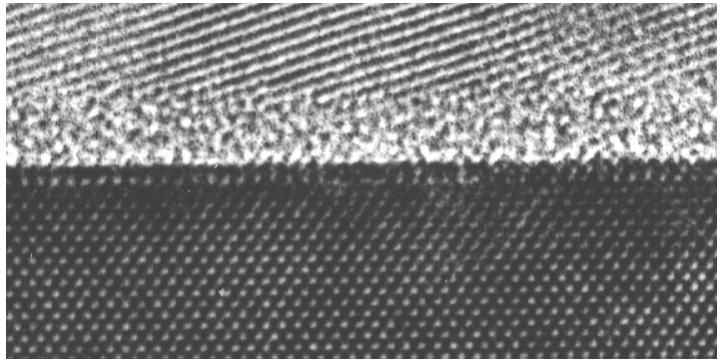

A transistor. (D.Muller et al, Lucent 2001).

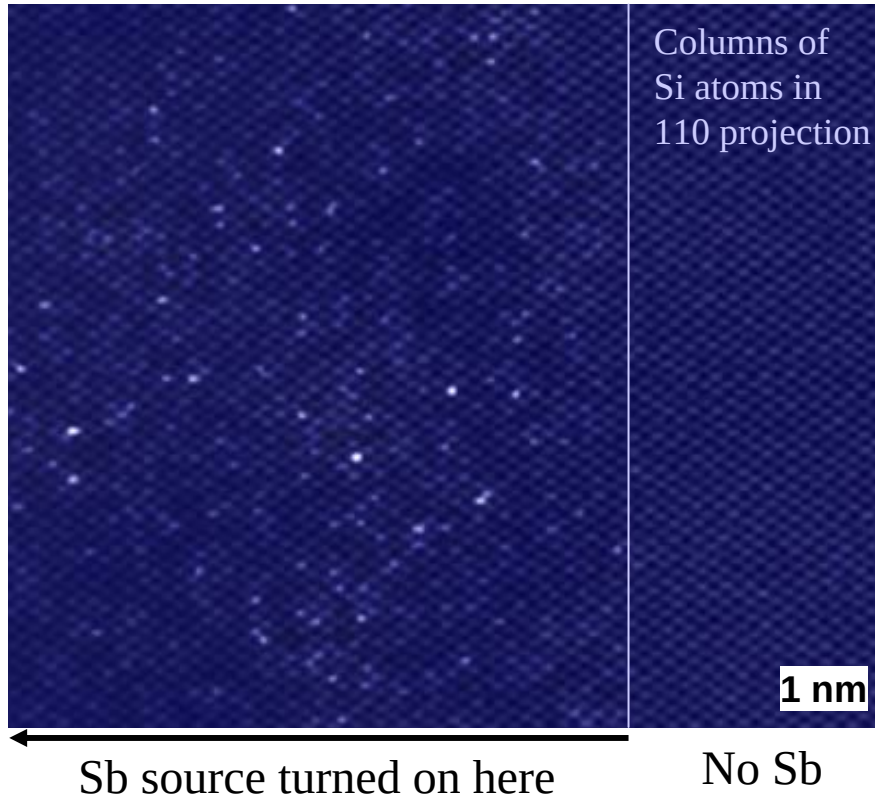

Individual dopant atoms within Si, seen in projection
(Nature, Voyles, Muller et al. Lucent, 2002)

In biology...

More contrast !

Protein synthesis (“Life itself”) in the Ribosome: The ribosome structure determined to 1nm resolution by TEM (tomographic cryomicroscopy). J.Frank et al.

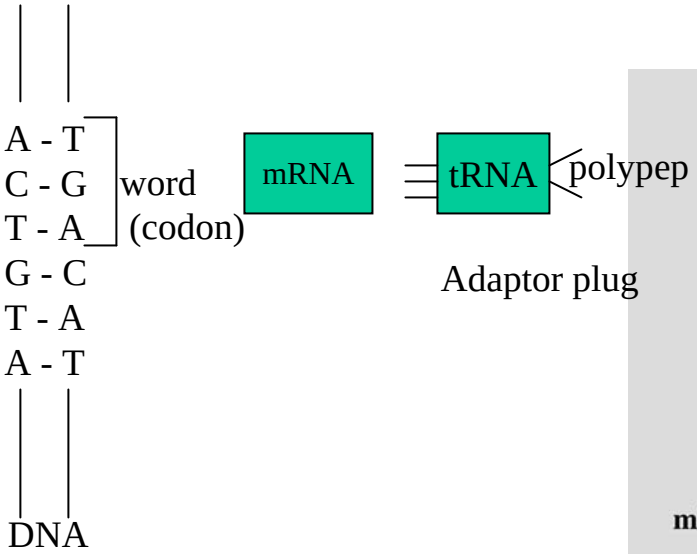

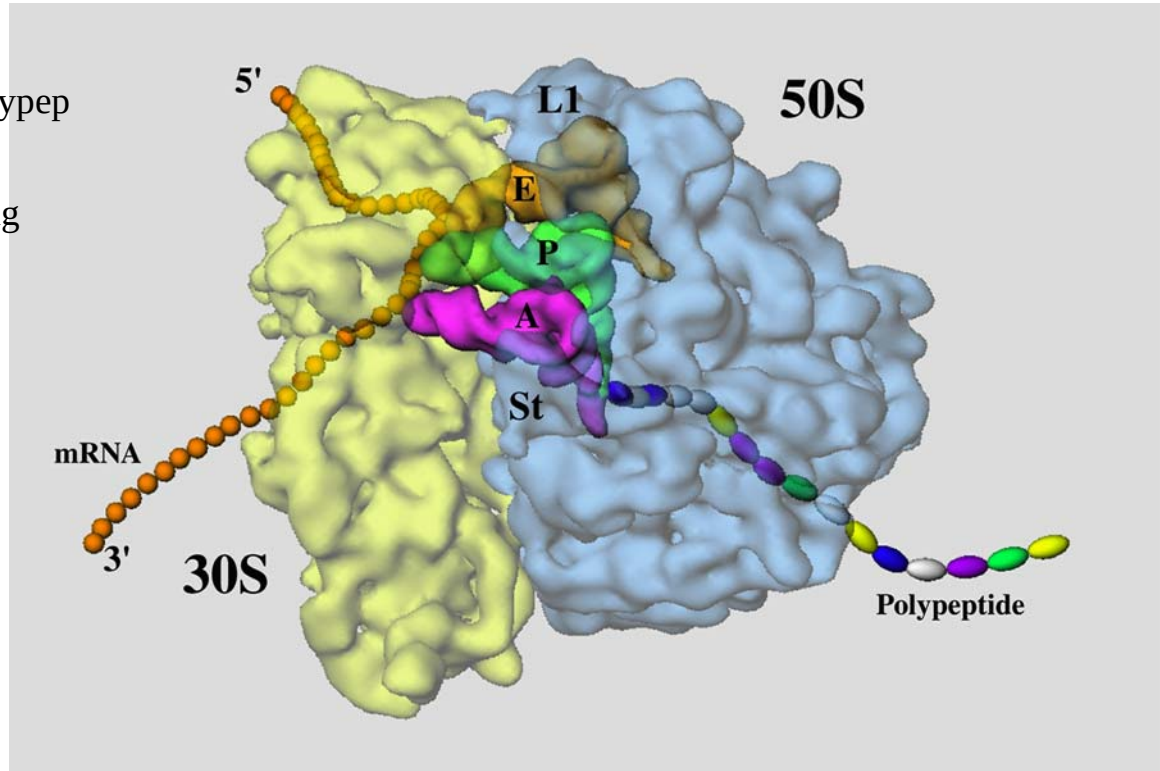

Ribosome width 25nm

(Frank et al Cell,100, p.537 (2000))

4 nucleic acids
2 (4) base pairs
mRNA reads one side only
3 pairs per word (per amino)
4^3 = 64 possibilities per amino
20 amino acids.
n words per gene (protein)

Experimental e-coli ribsome reconstuction from TEM images of non-crystallised mols in ice. mRNA bring 3-bit codons from DNA. tRNA “adaptors” (E,P,A) have plugs at one end to mRNA codon, at the other to an amino acid, which is added to the polypetide chain as the ribo runs along the mRNA. Chain will fold to become a new protein. (also Baumeister).

TABLE 1. Comparison of synchrotron soft X-ray and field-emission electron sources. All values are for 500 eV X-rays, or the 300 keV electron beams which are typically used to study ELNES at around 500 eV. ELNES uses parallel detection, XANES serial.

	ALS Undulator U5	e^- Cold FEG at 300 kV
Brightness	6.9 X 10^{24} particles /sec /cm^2 /sr /eV (1.1 X 10^{19} Ph/s /mm^2 /mr^2/ 0.1%BW)*	1.3 X 10^{29} particles /sec /cm^2 /sr /eV (6 X 10^9 A/cm^2 /sr.)
Degeneracy δ	18	1.54 X 10^{-5}
Coherent flux j_c	2.0 X 10^7 ph/s/0.1%BW	
Energy spread ΔE (un-monochromated).	4.6 eV	0.28 eV
Source size.	307x23 μm	2nm
Resolution of focussing element.	30 nm	0.1 nm
Flux into focussed probe	4.0 x 10^5 ph/s/0.1%BW	1nA into 1nm diameter. Higher with aberration corrector.

* This is the long time average value. Instantaneous values are about D=100 times greater.

Electron brightness values from Speidel et al Optik 49, 173. Nanotip at RT is 55 times brighter (Qian, Scheinfein, Spence J.Appl Phys.73, p.7041.

Spence and Howells, Ultramic.93, p.213 (2003) .

C XDI experiments with soft X-rays at ALS LBL.

E = 588 eV
2.1nm wavelength

Undulator
Zone-plate mono

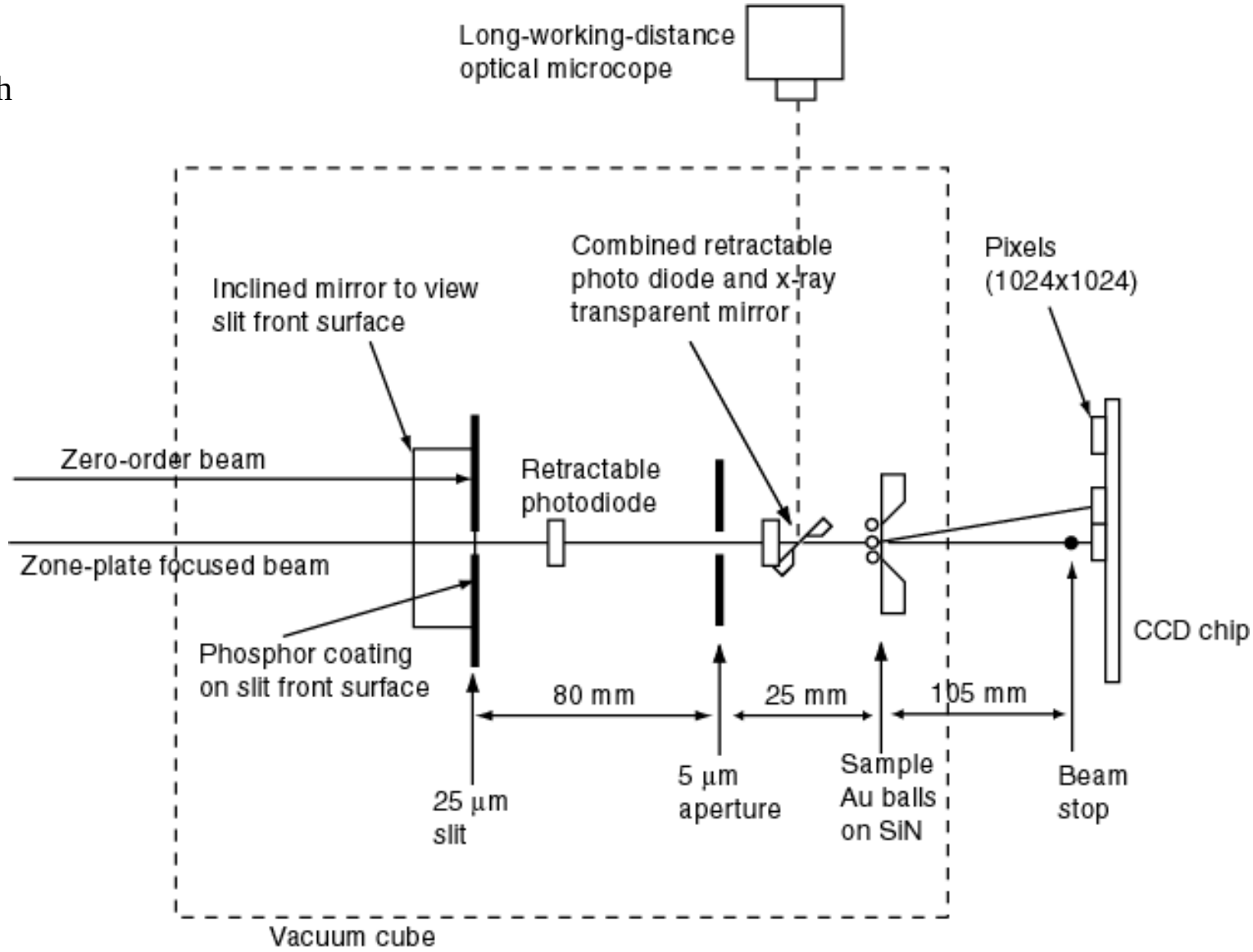

He, Howells, Weierrstall, Spence Chapman, Marchesini et al. Acta A59, 143. 03 .

HiO algorithm requires boundary of isolated object to be approx known. Estimate this from autocorrelation fn.

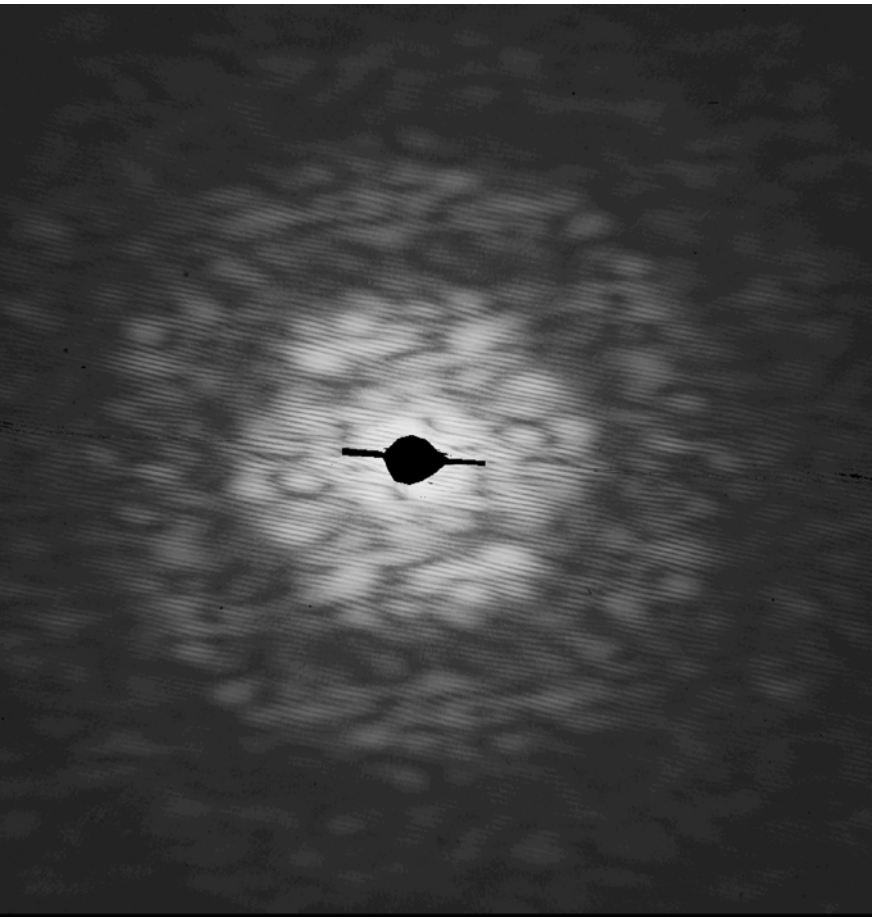

Soft X-ray transmission pattern at 588eV from cluster of **gold balls on SiN**.(Phase objects. Diam d=50nm)
First minimum is at $\sin\theta/\lambda = 1.394/d$. $\lambda = 2.1$nm

"Airey's disk" from one phase ball
Fringes due to interference between different balls

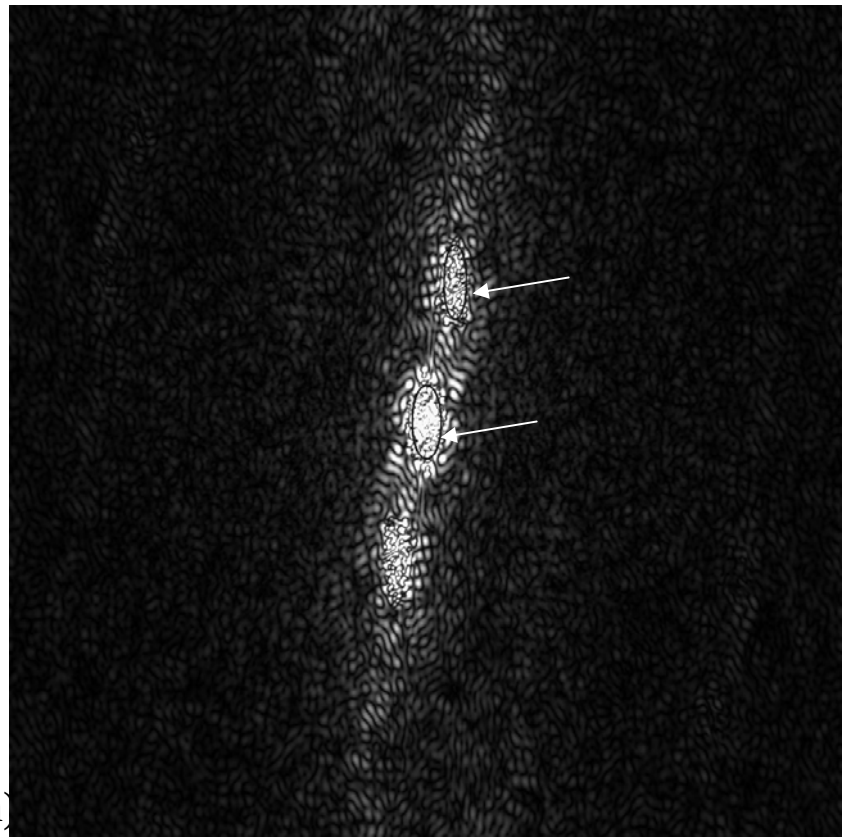

Autocorrelation (Patterson) function showing two ellipses used to define the acentric support.

Phase shift is 0.36 Rad per 30nm thickness at 588 eV.

Successful reconstruction of image from soft X-ray speckle alone.

SEM Image

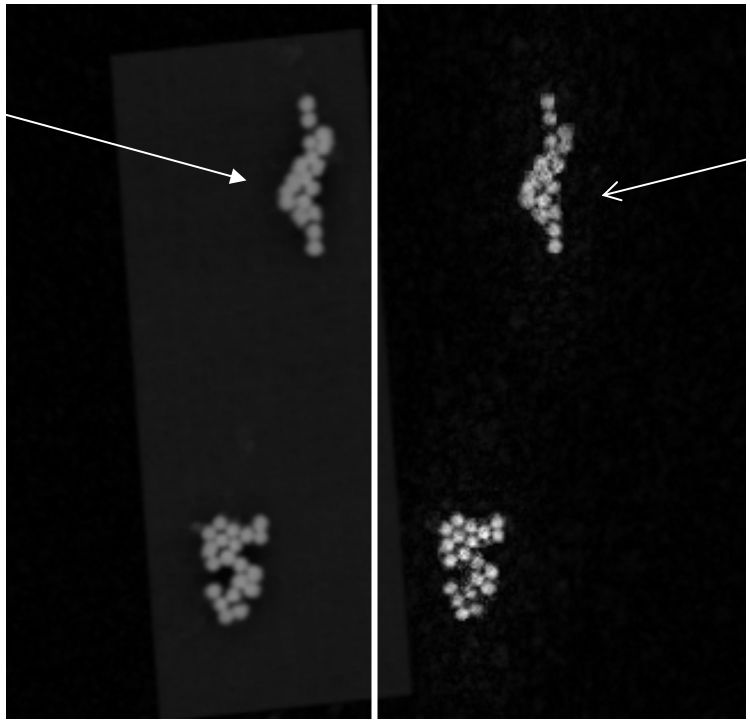

X-ray reconstruction

50nm diam. Gold Balls on transparent SiN membrane.

No “secondary image” was used - beyond "phase extension".

Approximate object boundary obtained from autocorrelation fn, "by hand".

How to make an isolated object ? Use AFM to remove unwanted balls.

(No density outside the reconstructed area L $=\theta_{min}/\lambda$ must contribute to the diffraction pattern).

He, Howells, Weierrstall, Spence Chapman, Marchesini et al. **Phys Rev B67, 174114. 03 .**

Is it possible to reconstruct without any knowledge of support ?

Get support of object from support of autocorrelation - then "shrink-wrap" to avoid previous subjective estimate of boundary.

Object estimate

Support estimate

50nm Gold Balls

λ=2.1nm

Notes:

First estimate of boundary (support) is boundary (4% threshold) of autocorr.

Autocorr is centric, object not.

Boundary of autocorr shrinks as HiO improves estimate. Every 20 itns make new support at 20% threshold.

Inversion symm eventually lost !

Intensity obscured by beamstop "floats" during iterations.

Cf Solvent flattening.

ALS LBL Expts LBL $

Marchesini,He,Howells,Chapman,Weierstall,Spence. Submitted. 2003 (PRB data).

Shrink-wrap simulations.
(Marchesini)

Recovered Image

Recovered support

Original object.

Greyscale bee.
(no "atomicity")

The noise level at which our algorithm fails to reconstruct occurs when the noise in real space becomes larger than the threshold used to update the support. Works better than HiO with loose support.

Tomography
-gold balls in 3D.

Complex 2D object with complex focussed probe.
Real part: - blue
+ red
Isolated by probe

Complex if large phase shifts, multiple scattering spatial variation of abs.

A different data set, showing "heavy-atom" method.

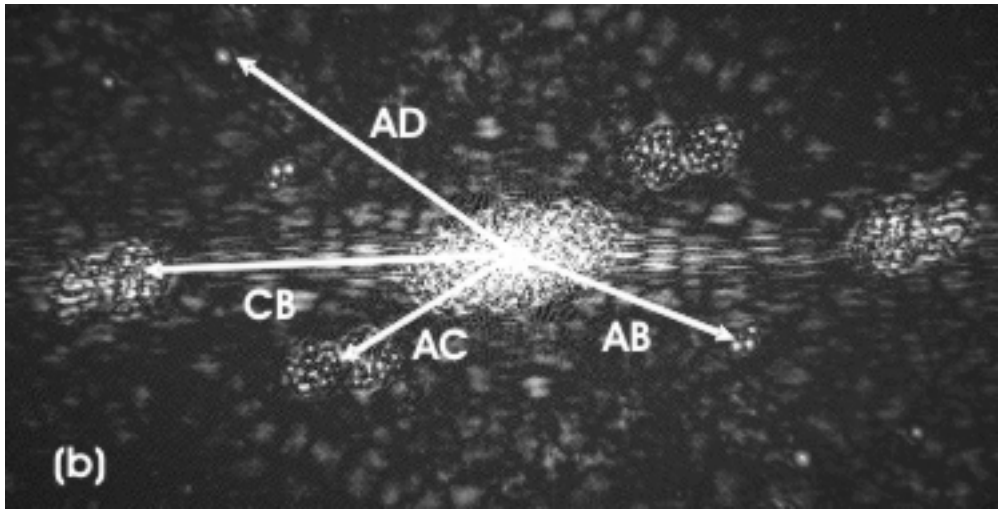

Autocorrelation from X-ray intensity
- a map of all interball vectors.

Friedel symm is a test for a real object.

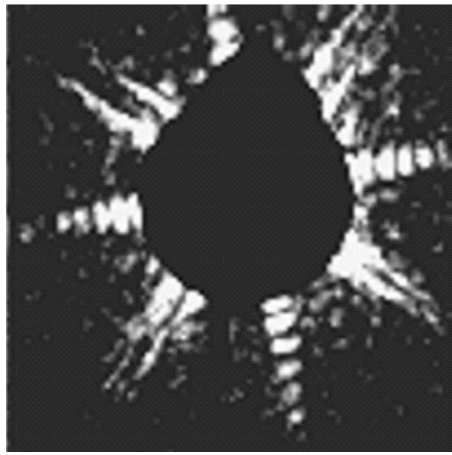

Sinc pattern from SiN window around beam stop.

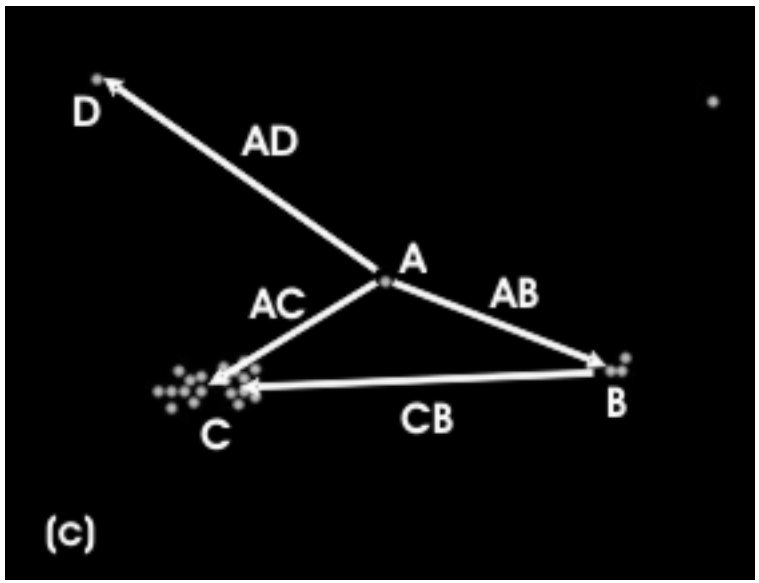

SEM real-space image

Note how balls at B are faithfully imaged in ball A in the autocorrelation function =ρ(r)*ρ(-r) at AB in figure (b)

This suggests using AFM to place single ball near unknown (eg cell). Autocorrelation then gives image and better support.

Support obtained from sem image.

Acta A.59, 143 (2003).

Diffraction from protein monolayers.

Compact support normal to a slab.

Oversampling along the beam direction in transmission geometry.

Two dimensional xtal gives redundancy against damage.

Membrane proteins, important for drug delivery, are hard to xtallize.

2. Oversampling along beam direction for monolayer protein crystals - lysozome.

Current practice in TEM **cryomicroscopy** is to record an image and a diffraction pattern for every tilt to solve the phase problem.Very difficult and tedious, especially at high angles.
Images are at <3 Ang resolution (resolves amino acids). Aberrations of lens must be deconvoluted.
Can HiO help by reducing the number of images needed for 3D phasing ?
Idea- Phase along rods with HiO. Link different rod phases with known phases from images.

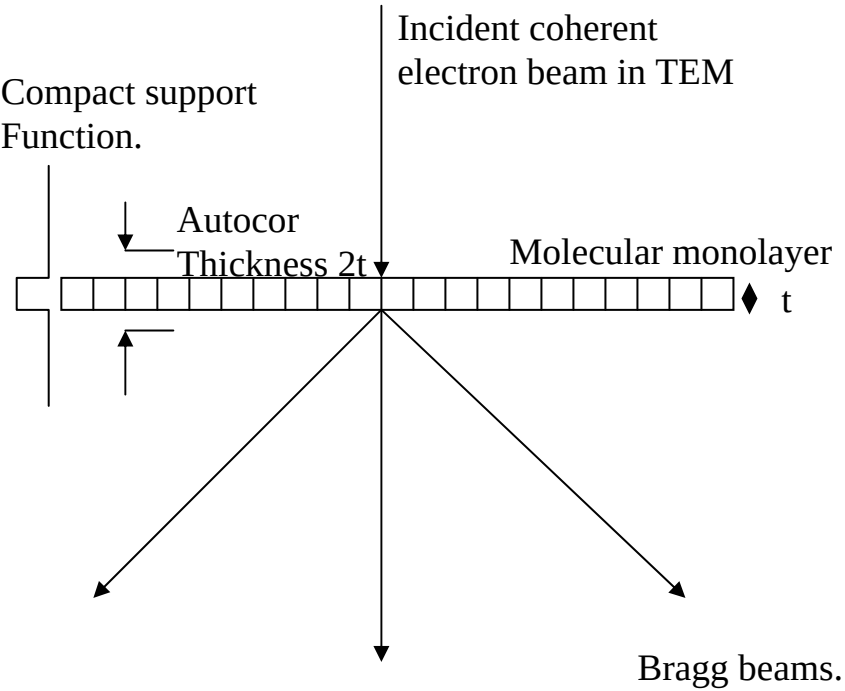

Real Space

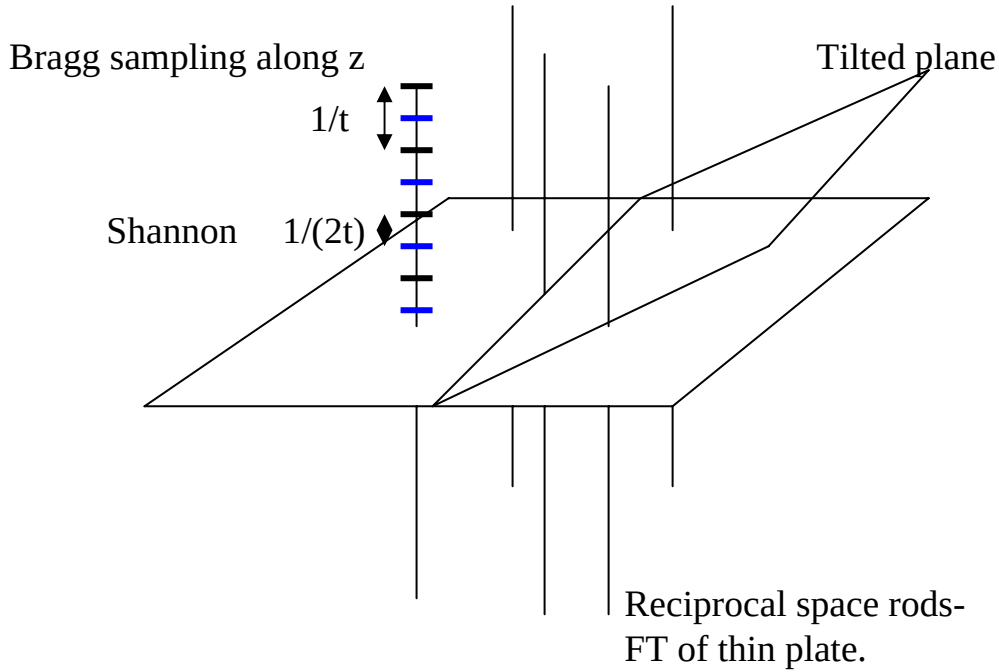

Reciprocal Space

Spence, Weierstall, Fricke, Downing, Glaeser. J. Struct. Biol. In press '03.

Tetracyanoethelene C_6N_4
Simulations for electron diffn.

To provide oversampling by three for the computational supercell, the unit cell was tripled in the direction normal to the slab, with vacuum on either side of the slab.

This object should be periodic laterally, to make an organic monolayer crystal.

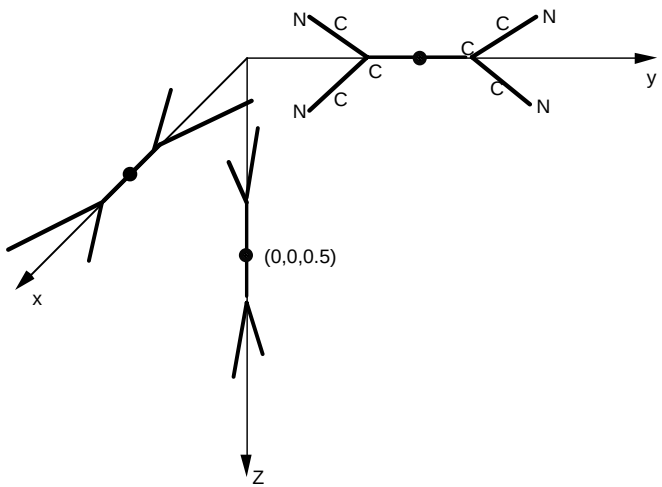

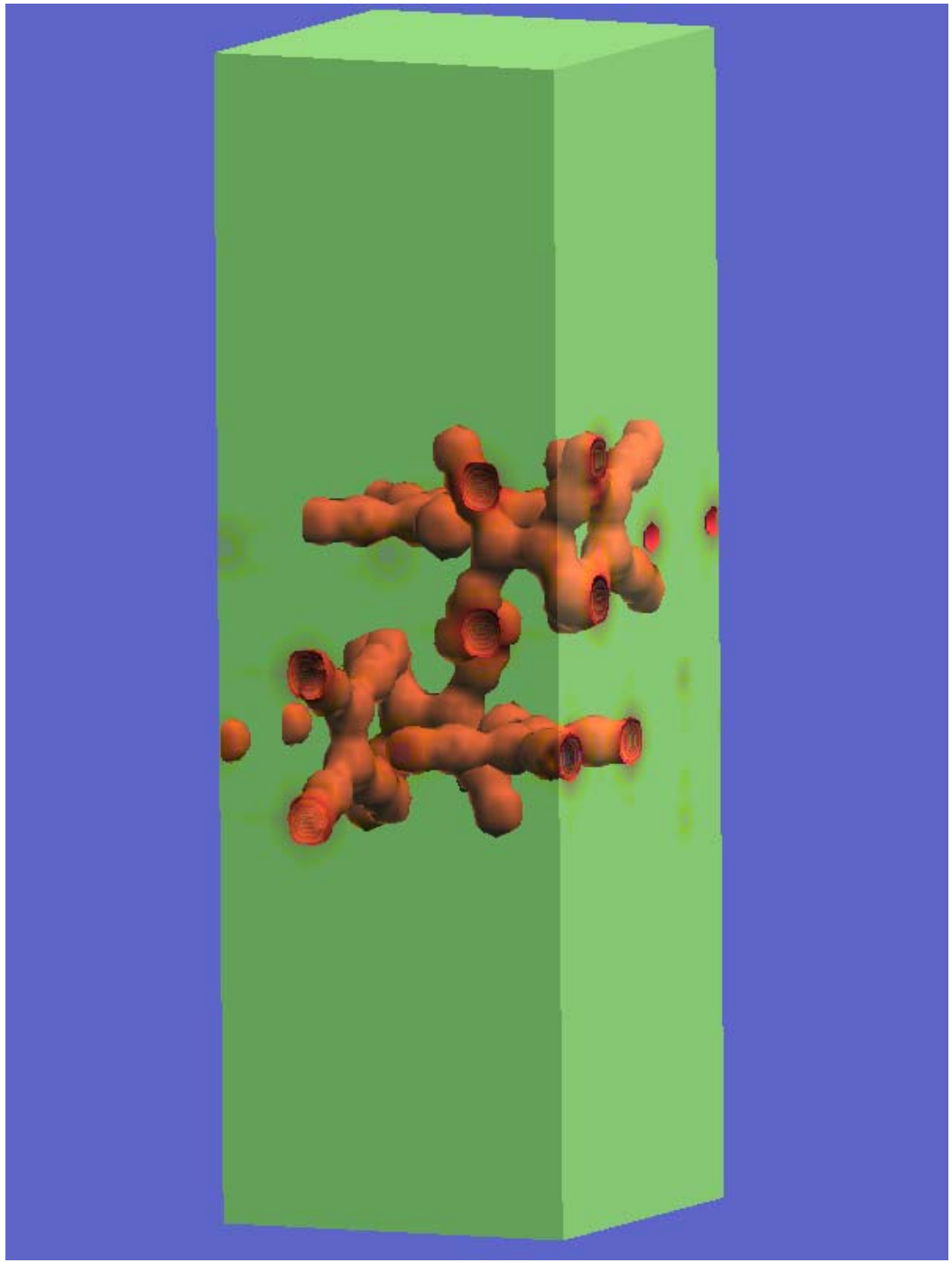

Result: Compact support along z for thin film will not solve phase problem alone - need some known phases.

The progress of the HiO* algorithm toward convergence is seen here in this real-space movie for tetracyanoethelene. Known phases were supplied on three planes.

The result is independent of the random choice of initial phases.

QuickTime™ and a
None decompressor
are needed to see this picture.

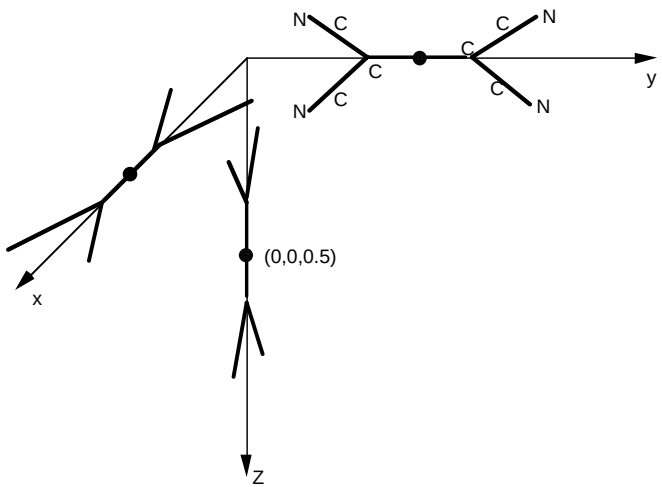

Tomographic HiO for organics using electron diffraction.

Find: Doesn't work unless some phases are given. HiO finds phases along beam dirn, not across.

Charge density for
Tetracyanoethelene C_6N_4
monolayer reconstructed by
HiO from simulated diffraction
intensity data to 0.35 Ang.
70 iterations. 30X30X90 voxel
Unit cell dims 0.97nm cubic.

Phases supplied on 3 planes in
reciprocal space.

QuickTime™ and a
Animation decompressor
are needed to see this picture.

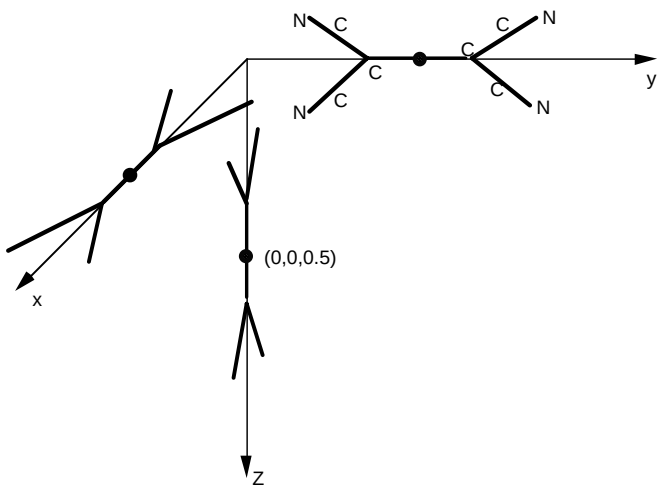

Test for lysozome protein (egg white). About 8,000 atoms, 53,000 Bragg beams.

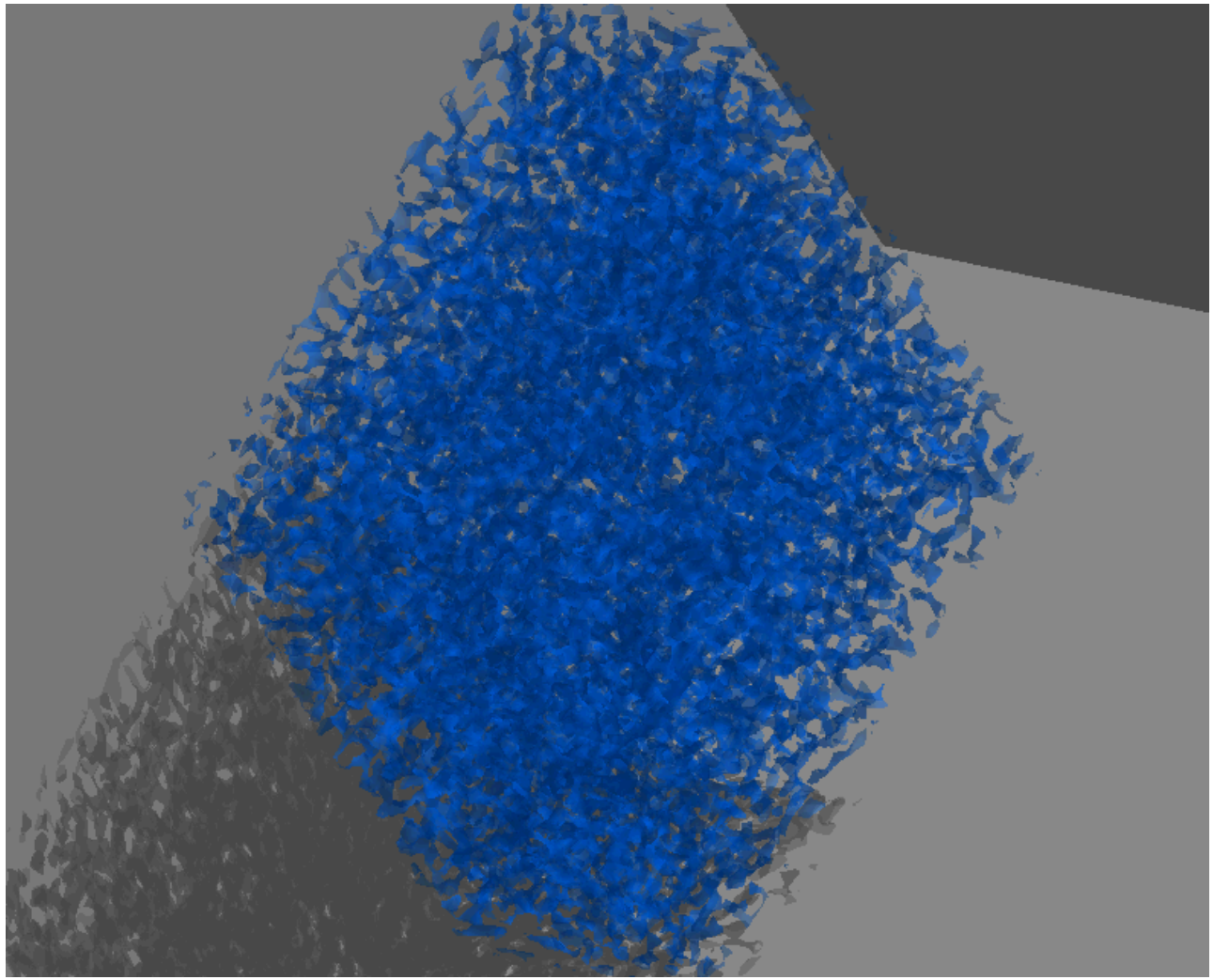

Isosurface map for the charge density of Lyzosome based on published atomic coordinates at 3 Angstrom resolution (identifies aminos).. The four-fold screw axis is seen in projection down the c axis. Tetragonal, P 43 21 2 a=79.1=b, c=37.9 Ang. Amino acids sequenced.

HiO for TEM Cryomicroscopy. Solving proteins hard to crystallize.

Results for Lysozome using 3D Braggs to 3 Ang. plus phases from images to 15 degrees.

Model Potential	HiO Reconstruction <15^{o} tilts, 105 iterns	HiO Recon. with noise R=25% Same images
	Corr Coeff=0.96	CC=0.95

54X54X78 voxels
To 3 Ang resolution
(identifies amino acids)
1 sec per itern. 100 iterns. Conclusion: method works well.

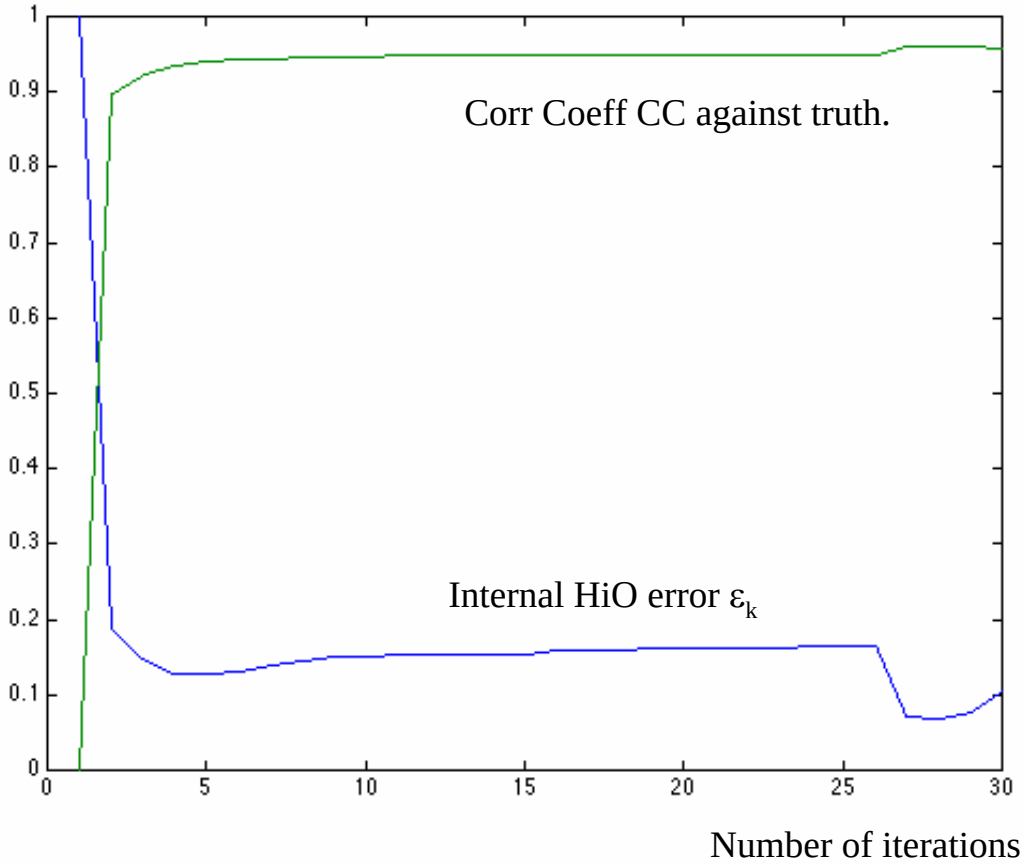

$$CC = \frac{\int_V \rho_t(\mathbf{r})\rho_e(\mathbf{r})d\mathbf{r}}{\left[\int_V \rho_t(\mathbf{r})^2 d\mathbf{r} \int_V \rho_e(\mathbf{r})^2 d\mathbf{r}\right]^{1/2}}$$

$$= \frac{\sum_{\mathbf{h}} |F_{\mathbf{h}}^t||F_{\mathbf{h}}^e| \cos(\phi_{\mathbf{h}}^t - \phi_{\mathbf{h}}^e)}{\left[\sum_{\mathbf{h}} |F_{\mathbf{h}}^t|^2 \sum_{\mathbf{h}} |F_{\mathbf{h}}^e|^2\right]^{1/2}}$$

$$= \frac{\sum_{\mathbf{h}} |F_h|^2 \cos(\phi_{\mathbf{h}}^t - \phi_{\mathbf{h}}^e)}{\sum_{\mathbf{h}} |F_{\mathbf{h}}|^2}$$

$$\varepsilon_k = \left(\frac{\sum_{(x,y)\notin S} |\tilde{g}_k(x,y,z)|^2}{\sum_{(x,y)} |\tilde{g}_k(x,y,z)|^2} \right)^{\frac{1}{2}}$$

Cross-correlation coefficient CC (upper curve) measuring agreement between model Lyzosome charge density and HiO estimate vs iteration number. No noise.

HiO error ε_k also shown (lower curve).

Four images tilted at 30 degrees, and four at 20 degrees used with axial image. Error decreases to 0.006.

For unknown structure, only ε_k is known, not CC ! (monotonic ?).

54X54X78 voxels
To 3 Ang resolution
(identifies amino acids)
1 sec per itern.100 itns.
(Mac,Matlab)

What is the smallest range of tilts from which image phases are needed ?

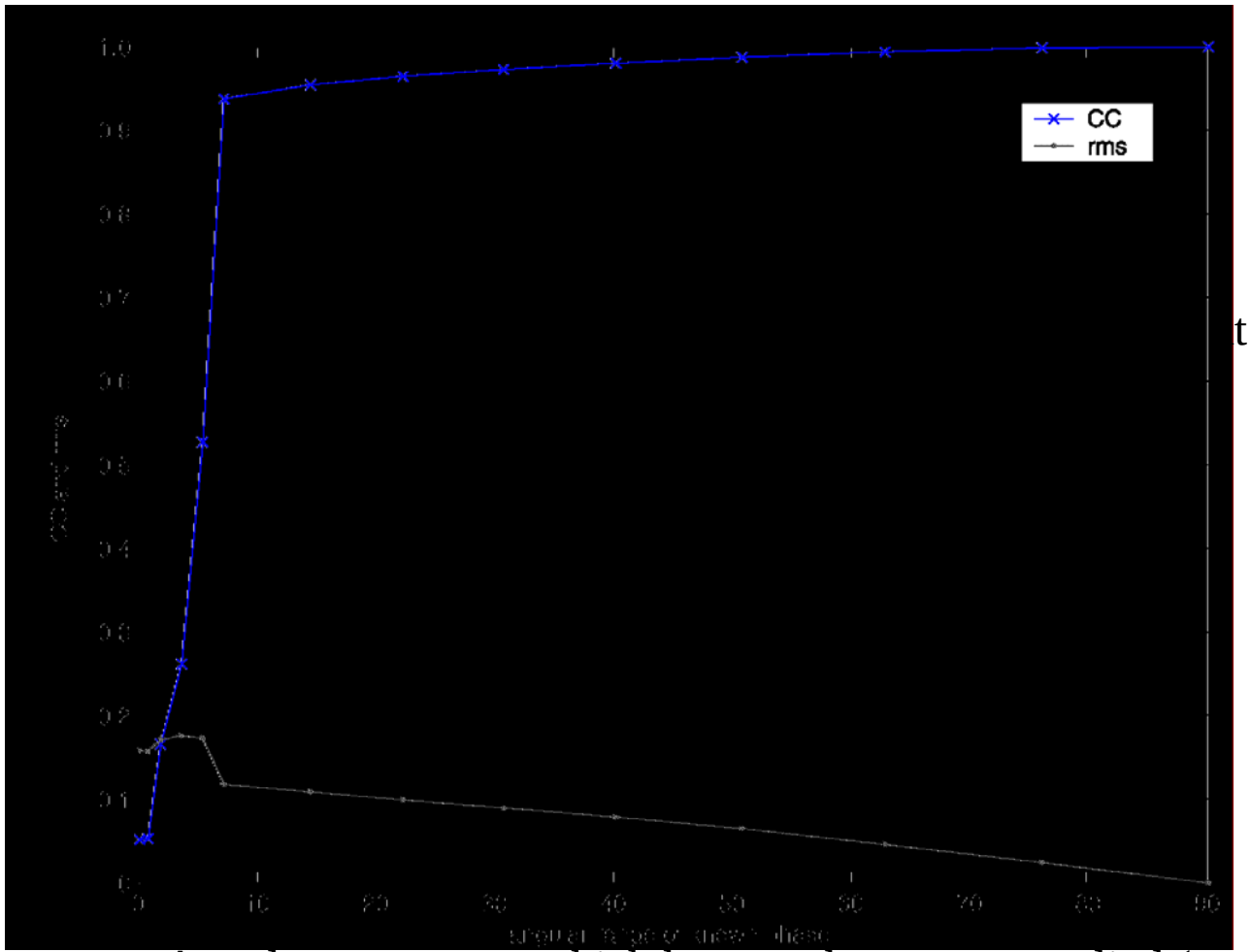

t which

Angular range over which known phases are supplied (random azimuth)

Correlation coefficient CC (upper curve) and rms error (lower curve) from HiO algorithm plotted against the angular range of reciprocal space, in degrees, within which known phases have been supplied to the algorithm.

Summary

1. Proteins which cannot be crystallized are very important
   (eg hard-to crystallize membrane proteins for drug delivery)

2. These can often be crystallized in two dimensions (eg on liquid surface etc).

3. Radiation damage prevents diffraction patterns being obtained for single isolated proteins.

4. Diffraction from two-dimensional "hydrated" proteins can be done in 3 dims.
   by cryo-tomographic TEM. Eg in amorphous ice.

5. This leaves a phase problem. Traditionally this has been solved by taking one image
   for each plane in diffraction space. Commonly need image tilts up to 80^o

6. By using the HiO iterative algorithm to oversample along the relps we can reduce the
   number of 0.3nm resolution images needed to phase the data from 100's to a few (eg $\pm 15^o$).
(0.3 nm is sufficient to distinguish the 20 amino acids, whose atomic structure is known).

7. Additional constraints have to be explored - Histogram, Bond-lengths, Sequence.

J.Spence, T.Fricke, R. Glaeser, K. Downing. J. Struct Biol. In press 03.

Hilbert Transforms - incorporation into HiO for "phase extension".

E.g. Kramers-Kronig relations, dispersion relations, multiple scattering analysis etc.

For a "causal" function f(r) s.t. f(r < 0) = 0, there is a simple relationship between the real and imag parts of F(u).

Apply this to an object density which is zero for r < 0 for some origin.

Apply it to a crystal (Mishnev, Acta A52, p.629 (1996))

It then generates the half-order Bragg reflections (from known *complex* Braggs) which would result if the molecule was surrounded by a vacuum jacket in a doubled cell. This satisfies Shannon, solves phase problem.

But we don't know the complex Braggs from the natural xtal !.

We have used this for phase extension. (Given image phases to some resolution, extend resolution by phasing additional higher-order Braggs). Mishnev obtains

$$F(h'+0.5,k'+0.5,l'+0.5) = \frac{1}{i\pi^3}\sum_{h,k,l}\frac{F(h,k,l)}{(h'-h+0.5)(k'-k+0.5)(l'-l+0.5)}$$

We now apply this a constraint in HiO, seeking the minimum number of low-resolution, known phases, needed for convergence.

Homometric structures.

One family of homometric structures (Acta Cryst 7, p. 237; Pauling's Bixbyite) may be generated using the result that…..

$$\rho_1(r) = l(r) * m(r)$$

and

$$\rho_2(r) = l(r) * m^*(-r)$$

have same Fourier modulus $|R(u)|$, *since*

$$R_1(u) = L(u)M(u) \quad and \quad R_2(u) = L(u)M^*(u)$$

If l(r) is a lattice and m(r) a molecule, then m, m* are enants, but ρ_1, ρ_2 are not enants.

Example:

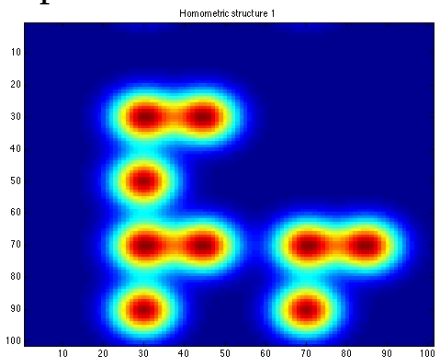

Homo1

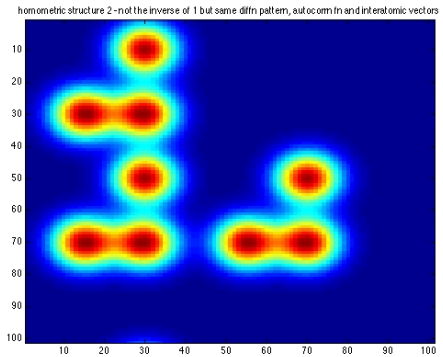

Homo2

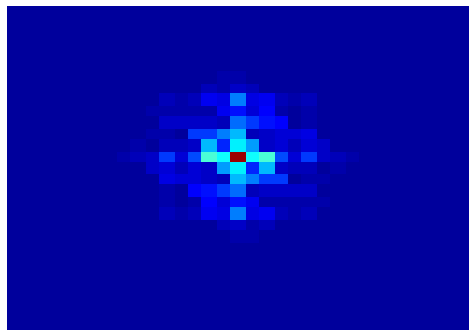

Fourier Mod of either

Note: Homo1 is not the inverse (enantiomorph) of Homo2.

Conclusion: HiO could not distinguish these unless tight support provided.

Distinguished by Multiple scattering ELNES

Coherence requirements for diffractive imaging.

Should spatial coherence width X_c equal width of object W or width of its autocorrelation function 2W ?
(this changes exposure time by 4 in 2D for fixed source brightness).

Moving from source point S_o to S_1 by α translates diffraction pattern by one detector pixel.
These source points are statistically independent, so coherence needed for DI is then lost.
(First-order Shannon sample excited by S_o coincides with zero order from S_1).

Shannon sampling requires pixel spacing $\alpha = \lambda/(2W)$

Van-Cittert Zernike gives $X_c=\lambda/\theta_C$

Combining these with $\theta_C < \alpha$ gives $\mathbf{X_c > 2W}$ (even for object in hole of diameter W !).

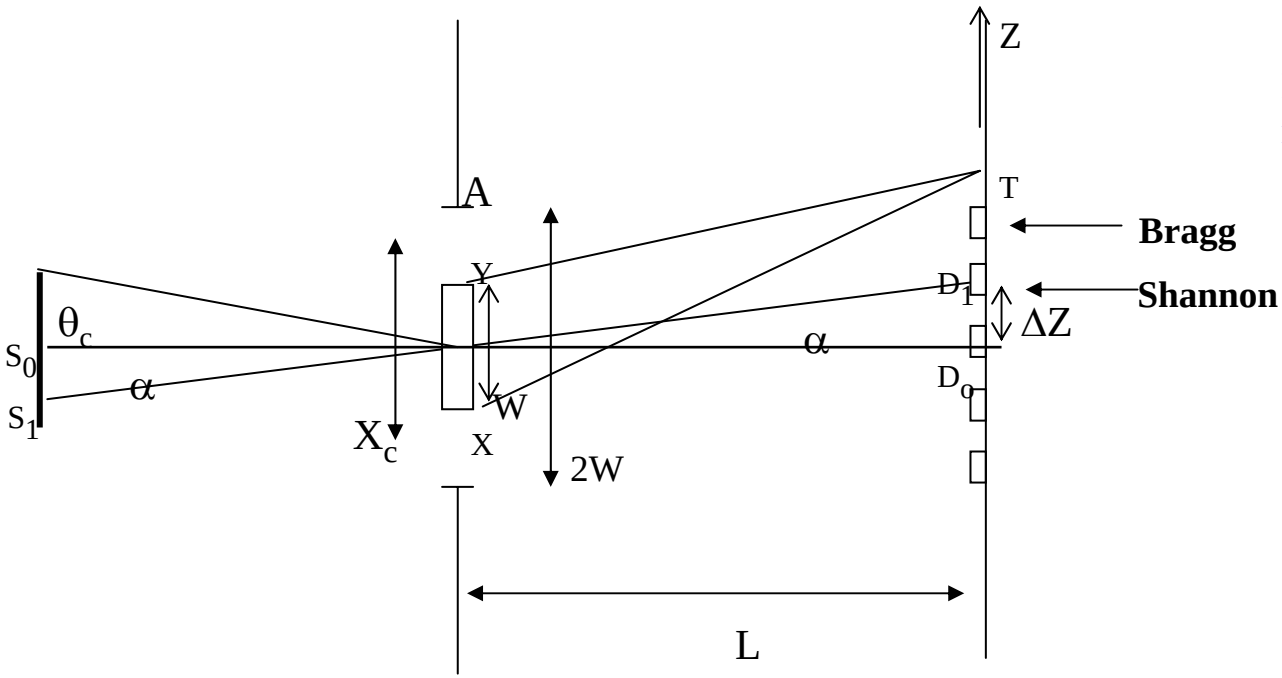

Nanoscience requires less, not more, coherence.

Temporal coherence:
Need $L=\lambda E/\Delta E > XT-YT$
or $L > W\,\theta_{max}$

or $\mathbf{N = W/d = 2E/\Delta E}$ **pixels**

The coherence volume in phase space is $N\,\lambda\,X^2_c$

Summary: α defines source size, and cannot exceed first-order Shannon sample at D_1.

HiO with small probes. Non-periodic object.

Can a coherent focussed beam be used to isolate a particle for HiO ?
Are coherent overlapping orders from xtal diffraction useful ?

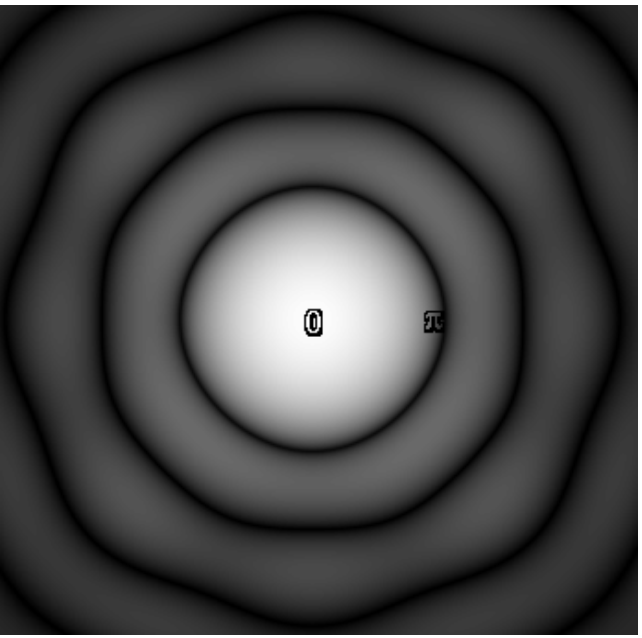

* Without aberrations, phase varies by π across focussed probe.
* Hence if particle smaller than probe, object may remain real.
*Then triangle support may work in 2D.

* For object comparable with probe size, in 2D, transmitted wave becomes complex. Use of known probe wavefunction as support is not successful. (first phase estimate is still random)

* For object comparable with probe size in 3D, have complex object. Shrink-wrap simulations worked.

Ptychography (greek "fold"). Periodic objects.

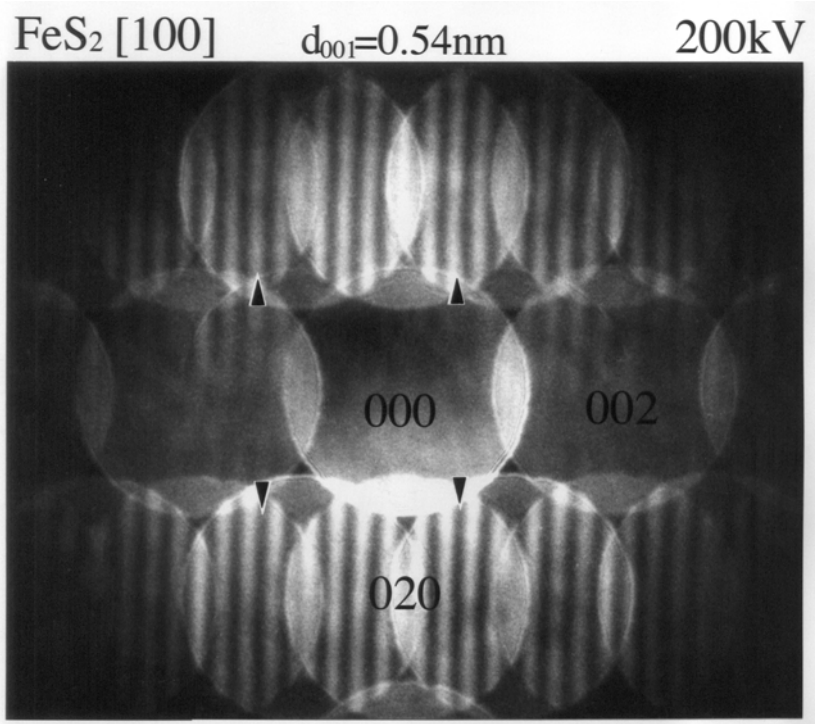

Experimental coherent electron diffraction with overlapping orders (STEM, Tanaka,Terauchi)

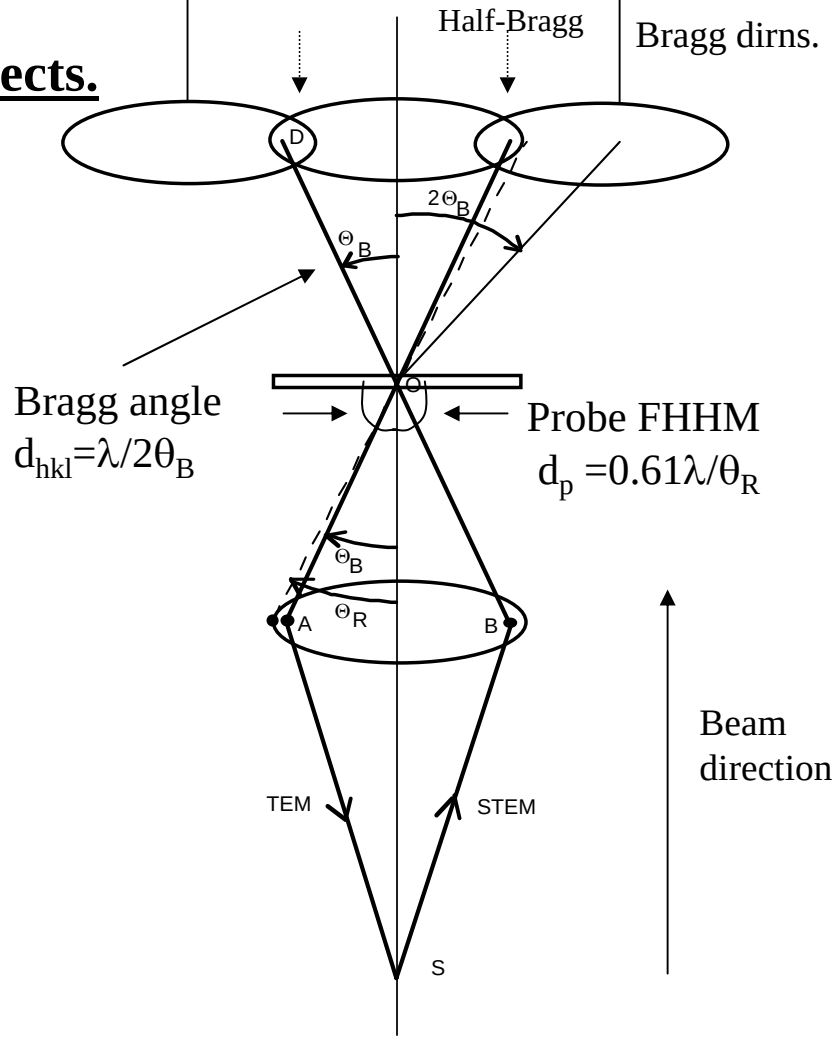

Set $d_p = d_{hkl}$ then $\theta_R = 1.2\ \theta_B$

Conclude: Need 20% overlap of coherent orders to match probe size to xtal spacing.

* Intensity at midpoint is indep of aberrations !
* Overlap is shadow image of crystal planes !
* Overlap is Fourier Image, periodic in defocus.
* Midpoint intensity varies sinusoidally with probe coord.
* If probe defocussed, pattern is in-line hologram.
* Super-resolution beyond info. limit by stepping out. (need only stability of first-order period).

Spence and Cowley, Optik, 50, p. 129. (1978)

Super-resolution through ptychography in STEM

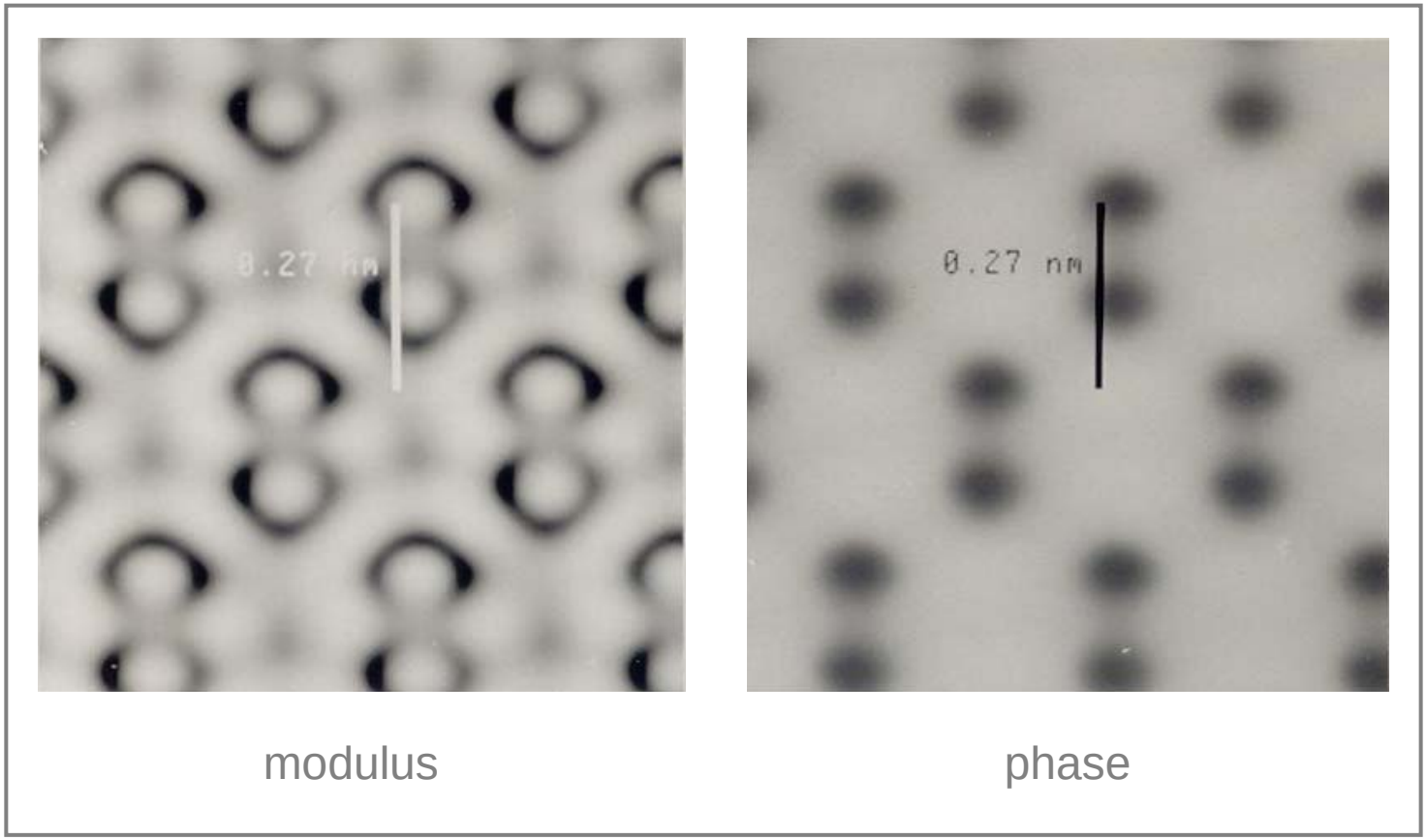

Atomic columns in a thin slab of silicon projected along [110]

Nellist, McCallum and Rodenburg, *Nature* **374** (1995) 630-632

The scope was a VG501, 100 kV, Cs = 3.1 mm, thus **WPOA point resolution is 4.2 angstroms**. Phase retrieval using ptychography was performed for all diffracted orders up to the 004 reflection (1.36 angstrom), which involves phasing 12 beams, and the data inverted to give the real-space image shown. The greyscale for the magnitude plot spans the range 22 (black) to 60 (white) in arbitrary units. For the phase the greyscale spans -104 degrees (black) to +38 degrees (white).

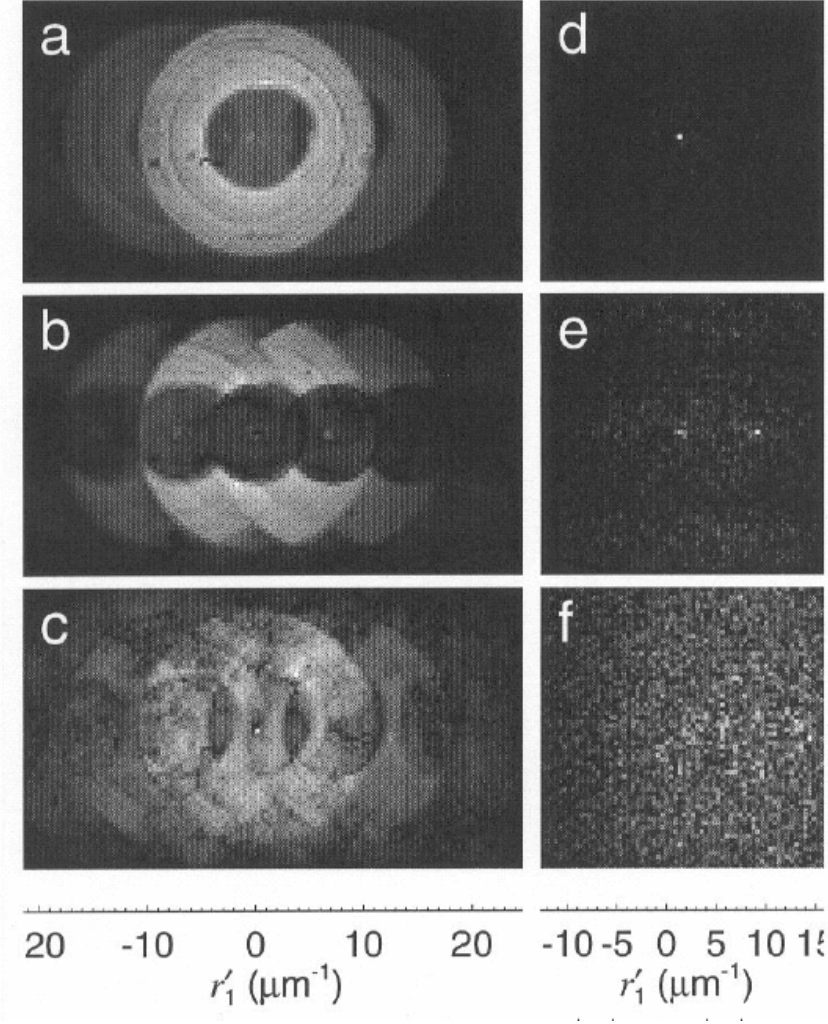

Coherent X-ray microdiffraction patterns from grating with overlap orders

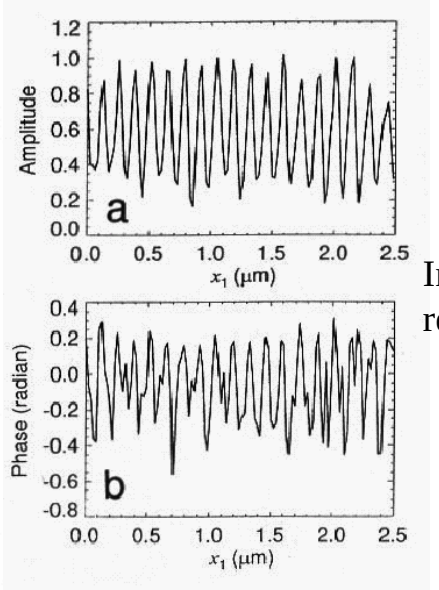

Image of grating (amp, phase) reconstructed from patterns

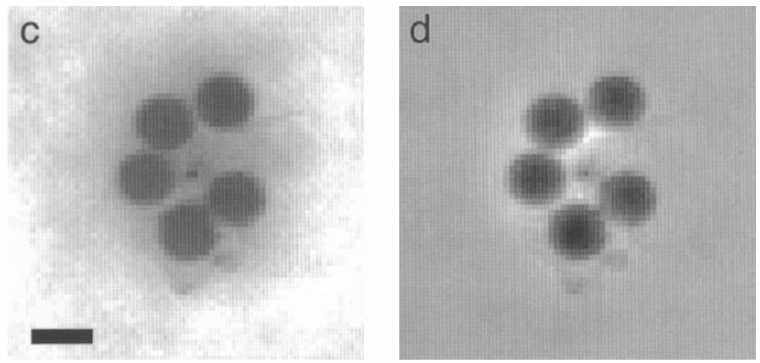

Ptychography for non-periodic object (Latex balls. Scale is 0.5 microns).

Ptychography with soft 3.2 nm X-rays. STXM used to give microdiffraction patterns.

H. Chapman. SEM 1997

Relationship between Ptychography and Diffractive Imaging.

Both depend on interference at "half-orders".

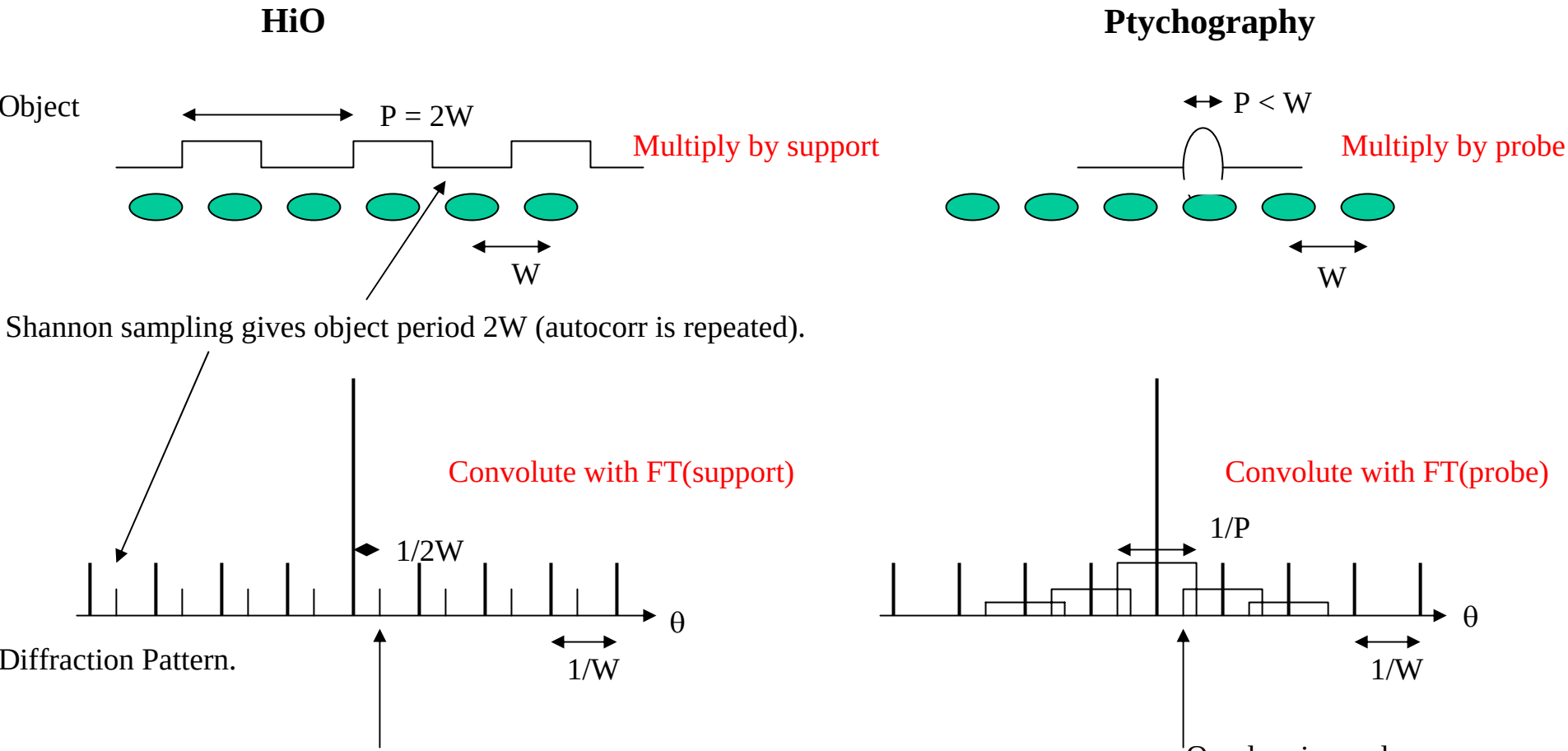

In HiO we multiply with something bigger than the object (the support) in real space to obtain interference at half-orders.

In Ptychog we multiply with something smaller (the probe) and get overlap, but the result depends on probe position.

Is atomic-resolution diffractive imaging possible with X-rays ?

Consider 10nm nanoparticle, HAP. Spring-8. **5 kV** Undulator, λ = 2 Ang, Si mono, zone-plate.

* After Si mono, flux is 10^{13} photons/sec.
*Rocking curve width for InSb nanodot is **12 millirads** for 10nm thickness.
*Cannot fill this with zoneplate, which limits divergence to 2mrad for 100nm outer zone.
*Horizontal divergence FWHM is 40 microradians, allowing X50 demag.
* Source size is 25 X 500 microns FWHM, becomes 0.5 X 10 microns.
*Flux into 10nm square is 10^{13} *0.01^2 /(0.5*10)=2X10^4 photons/sec.
*Diffraction efficiency for 10nm thickness is 3.4 X 10^{-4},
* This gives **7 X 10^4 photons/sec into (111) at 2 mRad** (more with worse mono).
*Spatial coherence needed for HiO is X_c = 20nm = $\lambda/\Delta\theta$, so need $\Delta\theta$ < 10 mRad (we have 2mR)
*Damage ? Cooling ? Better with TEM tomog ?

How to fake atomic resolution now…..

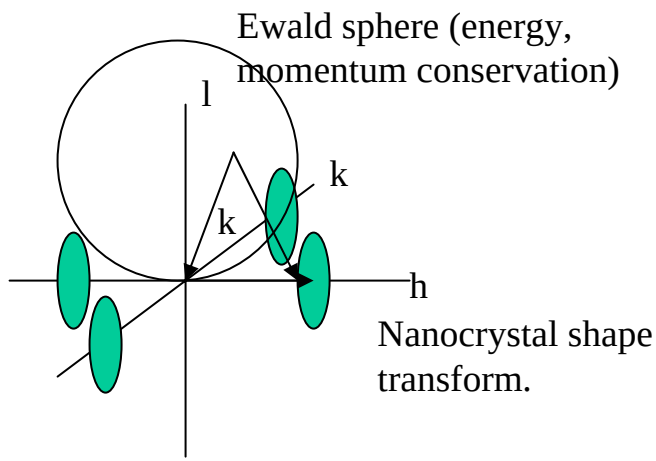

Eg **Robinson, Vartanyants et al PRL 87, 195505 (2001).**

Challenges:

1. Getting sufficient coherent photons

Analysis of recent ALS 9.0.1 experiment (588eV):

- Exposure that took 3 hours on 9.0.1, (10 nm resolution)
- Should have taken 5.27 min (with zone plate mono built to spec)
- Should take 0.31 min with current ALS,
  (U5.0 undulator, better beamline)
- should take 0.8 sec on upgraded ALS.

2. Choice of energy

- Reconstruction of real objects is easier.
- Electron density becomes more nearly real as energy increases.
- Exposure time scales as E^4 . (Coherent flux for fixed brightness scales as E^{-2}, and cross section scales as E^{-2})
- Best compromise specimen dependent 0.5 – 4 KeV for storage ring
- Damage is the key. Need maximum elastic per inelastic scattering.

DOSE and FLUX SCALING WITH RESOLUTION

M. Howells et al. calculated the coherent scattering cross section of a cubic voxel and thence the dose D required to produce P scattered x-rays into a detector with collection angle chosen for resolution d with the following result

$$D = \frac{\mu P h\nu}{\varepsilon} \frac{1}{r_e^2 \lambda^2 |\rho|^2 d^4} \qquad \text{Flux} = \frac{P}{r_e^2 \lambda^2 |\rho|^2 d^4}$$

μ = the voxel intensity absorption coefficient
$h\nu$ = the photon energy
r_e = the classical electron radius
λ = the photon wave length
ρ = the scattering strength of the voxel material in electrons per unit volume
ε = the density

The dose scales as the inverse fourth power of the resolution

Dose vs resolution

25 xrays per pixel

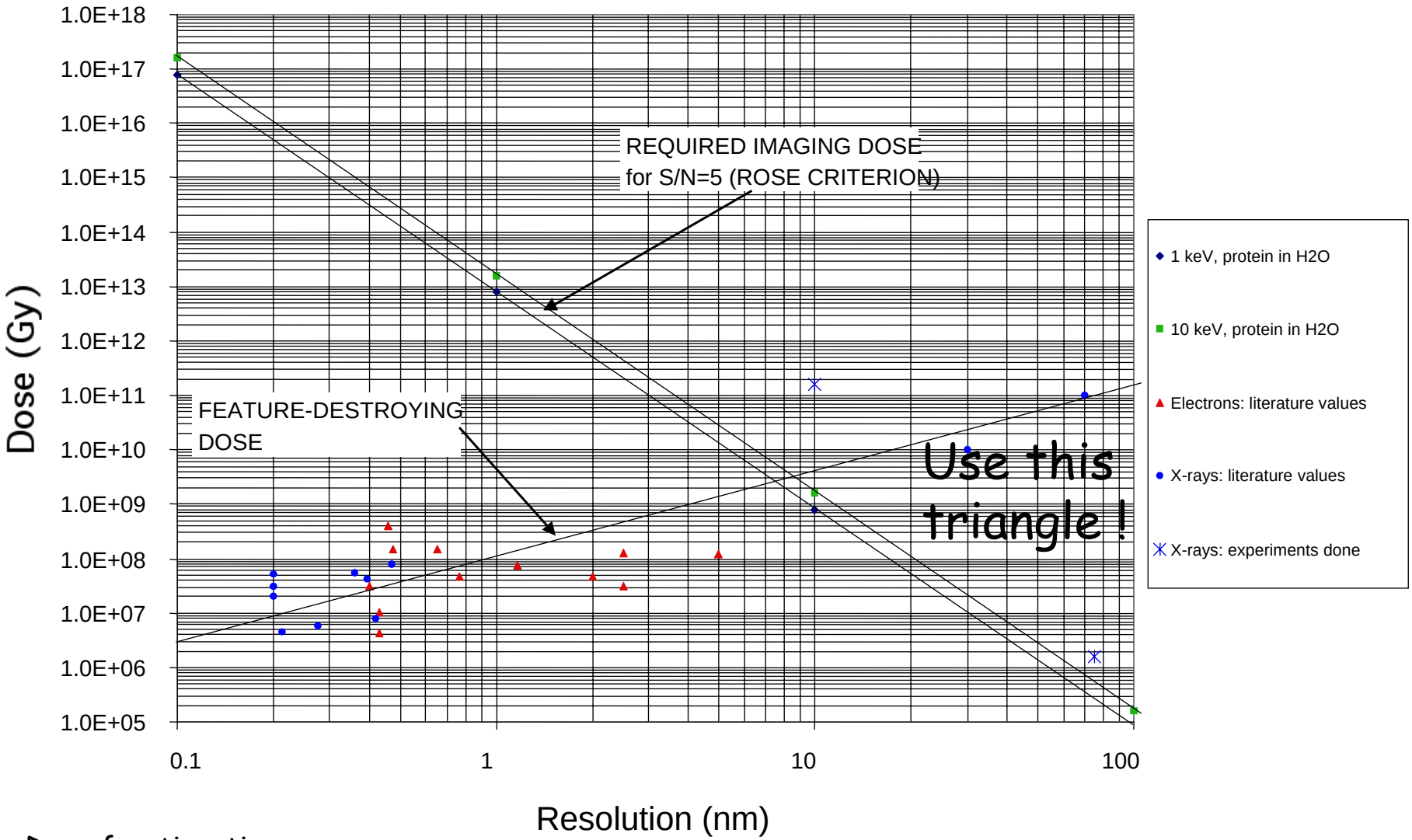

Dose fractionation
(Hegerl and Hoppe 1976, McEwen 1995)

Conclude: 10nm is max resolution possible (organics)
Howells, Kirz, Padmore, Tanuma, Spence, He et al '03

Summary of potential applications for CXDI.

1. Materials Science.

In the 0.5-4kV range: 2nm resolution aim.

i) Visualization of the internal labyrinth structure of the new mesoporous framework structures, (eg glassy foams), molecular sieves and possibly hydrogen storage (large internal surface area).

ii). The imaging of aerosols.

iii) Imaging the complex tangles of dislocation lines which are responsible for work-hardening, not presently understood.

iv) Imaging the cavities within duplex steels, which provide very high uniform extension (>500% percent).

v). Magnetic multilayers may be imaged in three-dimensions, thus revealing their defect structure.

vi). The tomographic imaging of misfit dislocations at interfaces, free of the thin-film elastic relaxation processes which distort the images obtained by TEM. These interface dislocations limit the performance of many electo-optic devices, and play a crucial role in thin-film crystal growth.

vii). Imaging of the three-dimensional arrangement of Orowan dislocation loops which , by entanglement with particles, provide the dispersion-hardening of copper alloys.

viii). The imaging of the complex tangle of fibres in fibre-composite materials.

ix). The imaging of precipitates in metal-matrix composite materials

x) Three dimensional internal imaging of semiconductor devices.

2. Biology.

i) Tomographic imaging of frozen hydrated cells in amorphous ice beyond the resolution of zone plates.

Small frozen hydrated cell, organelle; see macromolecular aggregates, organisation of mols in cell.

10nm resolution aim. 1-10 microns thick. (CryoTEM has multiple scattering above 0.5 microns).

ii) Chemical mapping of labels ?

Summary - Coherent Diffractive Imaging (CDI)

*Membrane proteins (important for drug delivery) are difficult to xtalize in 3D. 2D xtals give immunity to damage - ideal for CDI tomog (electrons , Xrays ?). Cryo gives "hydration"

*By using the HiO iterative algorithm to oversample along the relps we can reduce the number of 0.3nm resolution images needed to phase the data from 100's to a few (eg $\pm 30^{o}$). (0.3 nm distinguishes the 20 aminos, of known structure). Data collection reduced from months.

*Our large-angle diffraction camera with HiO data analysis forms a new type of **diffraction-limited, aberration-free tomographic** microscope. "**Shrink-wrap**" - no support.

*Large NA in CDI makes more efficient use of damaging radiation. Reconstruction from 3D data avoids depth-of-field limitation of zone-plate tomography. Focused illumination will allow selection of one or two-part (complex) objects from a field.

*Dose scales as $(\text{resolution})^{-4}$. Measurements show that images of cells should be obtainable at 10 nm resolution, 0.5-10 μm thickness, by soft X-rays at 100 K.

*Imaging by harder coherent X-rays of inorganic nanostructures (such as mesoporous materials, aerosols and catalysts) at perhaps 2 nm resolution or better can be expected.(Robinson..)

*Imaging with new radiations for which no lenses exist, and single molecule imaging with X-ray free-electron laser pulses remain to be explored (Chapman...).

S.Marchesini, H.He, M.Howells, U.Weierstall, H.Chapman, J.C. Spence. LBL/ASU DOE, ARO $

Appendices.